# The Chemistry and Applications of Metal-Organic Frameworks

Hiroyasu Furukawa *et al.*

*Science* **341**, (2013);
DOI: 10.1126/science.1230444



*Science* (print ISSN 0036-8075; online ISSN 1095-9203) is published weekly, except the last week in December, by the American Association for the Advancement of Science, 1200 New York Avenue NW, Washington, DC 20005. 

# The Chemistry and Applications of Metal-Organic Frameworks

Hiroyasu Furukawa, Kyle E. Cordova, Michael O'Keeffe, Omar M. Yaghi*

READ THE FULL ARTICLE ONLINE
http://dx.doi.org/10.1126/science.1230444

Cite this article as H. Furukawa *et al.*, *Science* **341**, 1230444 (2013).
DOI: 10.1126/science.1230444

**Background:** Metal-organic frameworks (MOFs) are made by linking inorganic and organic units by strong bonds (reticular synthesis). The flexibility with which the constituents' geometry, size, and functionality can be varied has led to more than 20,000 different MOFs being reported and studied within the past decade. The organic units are ditopic or polytopic organic carboxylates (and other similar negatively charged molecules), which, when linked to metal-containing units, yield architecturally robust crystalline MOF structures with a typical porosity of greater than 50% of the MOF crystal volume. The surface area values of such MOFs typically range from 1000 to 10,000 $m^2/g$, thus exceeding those of traditional porous materials such as zeolites and carbons. To date, MOFs with permanent porosity are more extensive in their variety and multiplicity than any other class of porous materials. These aspects have made MOFs ideal candidates for storage of fuels (hydrogen and methane), capture of carbon dioxide, and catalysis applications, to mention a few.

**Advances:** The ability to vary the size and nature of MOF structures without changing their underlying topology gave rise to the isoreticular principle and its application in making MOFs with the largest pore aperture (98 Å) and lowest density (0.13 $g/cm^3$). This has allowed for the selective inclusion of large molecules (e.g., vitamin $B_{12}$) and proteins (e.g., green fluorescent protein) and the exploitation of the pores as reaction vessels. Along these lines, the thermal and chemical stability of many MOFs has made them amenable to postsynthetic covalent organic and metal-complex functionalization. These capabilities enable substantial enhancement of gas storage in MOFs and have led to their extensive study in the catalysis of organic reactions, activation of small molecules (hydrogen, methane, and water), gas separation, biomedical imaging, and proton, electron, and ion conduction. At present, methods are being developed for making nanocrystals and supercrystals of MOFs for their incorporation into devices.

**Outlook:** The precise control over the assembly of MOFs is expected to propel this field further into new realms of synthetic chemistry in which far more sophisticated materials may be accessed. For example, materials can be envisaged as having (i) compartments linked together to operate separately, yet function synergistically; (ii) dexterity to carry out parallel operations; (iii) ability to count, sort, and code information; and (iv) capability of dynamics with high fidelity. Efforts in this direction are already being undertaken through the introduction of a large number of different functional groups within the pores of MOFs. This yields multivariate frameworks in which the varying arrangement of functionalities gives rise to materials that offer a synergistic combination of properties. Future work will involve the assembly of chemical structures from many different types of building unit, such that the structures' function is dictated by the heterogeneity of the specific arrangement of their constituents.

## ARTICLE OUTLINE



## SUPPLEMENTARY MATERIALS

Materials and Methods
Figs. S1 to S8
Tables S1 to S5
References (*135–363*)
Related Web sites
Cambridge Structural Database reference codes for MOFs

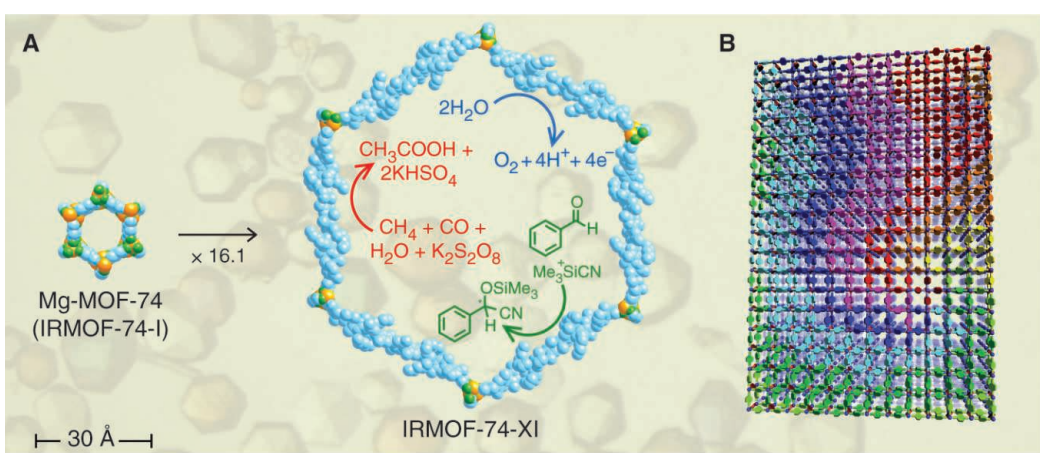


**Metal-organic framework (MOF) structures are amenable to expansion and incorporation of multiple functional groups within their interiors.** (**A**) The isoreticular expansion of MOFs maintains the network's topology by using an expanded version of the parent organic linker. Examples of catalysis in MOFs are shown in the large space created by IRMOF-74-XI; Me is a methyl group. (**B**) Conceptual illustration of a multivariate MOF (MTV-MOF) whose pores are decorated by heterogeneous mixtures of functionalities that arrange in specific sequences. (**Background**) Optical image of zeolitic imidazolate framework (ZIF) crystals.

The list of author affiliations is available in the full article online.
*Corresponding author. E-mail: yaghi@berkeley.edu

# The Chemistry and Applications of Metal-Organic Frameworks

Hiroyasu Furukawa,[1,2] Kyle E. Cordova,[1,2] Michael O'Keeffe,[3,4] Omar M. Yaghi[1,2,4]*

Crystalline metal-organic frameworks (MOFs) are formed by reticular synthesis, which creates strong bonds between inorganic and organic units. Careful selection of MOF constituents can yield crystals of ultrahigh porosity and high thermal and chemical stability. These characteristics allow the interior of MOFs to be chemically altered for use in gas separation, gas storage, and catalysis, among other applications. The precision commonly exercised in their chemical modification and the ability to expand their metrics without changing the underlying topology have not been achieved with other solids. MOFs whose chemical composition and shape of building units can be multiply varied within a particular structure already exist and may lead to materials that offer a synergistic combination of properties.

The past decade has seen explosive growth in the preparation, characterization, and study of materials known as metal-organic frameworks (MOFs). These materials are constructed by joining metal-containing units [secondary building units (SBUs)] with organic linkers, using strong bonds (reticular synthesis) to create open crystalline frameworks with permanent porosity (*1*). The flexibility with which the metal SBUs and organic linkers can be varied has led to thousands of compounds being prepared and studied each year (Figs. 1 and 2). MOFs have exceptional porosity and a wide range of potential uses including gas storage, separations, and catalysis (*2*). In particular, applications in energy technologies such as fuel cells, supercapacitors, and catalytic conversions have made them objects of extensive study, industrial-scale production, and application (*2*–*4*).

Among the many developments made in this field, four were particularly important in advancing the chemistry of MOFs: (i) The geometric principle of construction was realized by the linking of SBUs with rigid shapes such as squares and octahedra, rather than the simpler node-and-spacer construction of earlier coordination networks in which single atoms were linked by ditopic coordinating linkers (*1*). The SBU approach not only led to the identification of a small number of preferred ("default") topologies that could be targeted in designed syntheses, but also was central to the achievement of permanent porosity in MOFs (*1*). (ii) As a natural outcome of the use of SBUs, a large body of work was subsequently reported on the use of the isoreticular principle (varying the size and nature of a structure without changing its underlying topology) in the design of MOFs with ultrahigh porosity and unusually large pore openings (*5*). (iii) Postsynthetic modification (PSM) of MOFs—incorporating organic units and metal-organic complexes through reactions with linkers—has emerged as a powerful tool for changing the reactivity of the pores (e.g., creating catalytic sites) (*6*). (iv) Multivariate MOFs (MTV-MOFs), in which multiple organic functionalities are incorporated within a single framework, have provided many opportunities for designing complexity within the pores of MOFs in a controlled manner (*7*).

Below, we focus on these aspects of MOF chemistry because they are rarely achieved in other materials and because they lead to the previously elusive synthesis of solids by design. Unlike other extended solids, MOFs maintain their underlying structure and crystalline order upon expansion of organic linkers and inorganic SBUs, as well as after chemical functionalization, which greatly widens the scope of this chemistry. We review key developments in these areas and discuss the impact of this chemistry on applications such as gas adsorption and storage, catalysis, and proton conduction. We also discuss the concept of MTV-MOFs in relation to the sequence of functionality arrangement that is influenced by the electronic and/or steric interactions among the functionalities. Highly functional synthetic crystalline materials can result from the use of such techniques to create heterogeneity within MOF structures.

## Design of Ultrahigh Porosity

During the past century, extensive work was done on crystalline extended structures in which metal ions are joined by organic linkers containing Lewis base–binding atoms such as nitriles and bipyridines (*8*, *9*). Although these are extended crystal structures and not large discrete molecules such as polymers, they were dubbed coordination "polymers"—a term that is still in use today, although we prefer the more descriptive term MOFs, introduced in 1995 (*10*) and now widely accepted. Because these structures were constructed from long organic linkers, they encompassed void space and therefore were viewed to have the potential to be

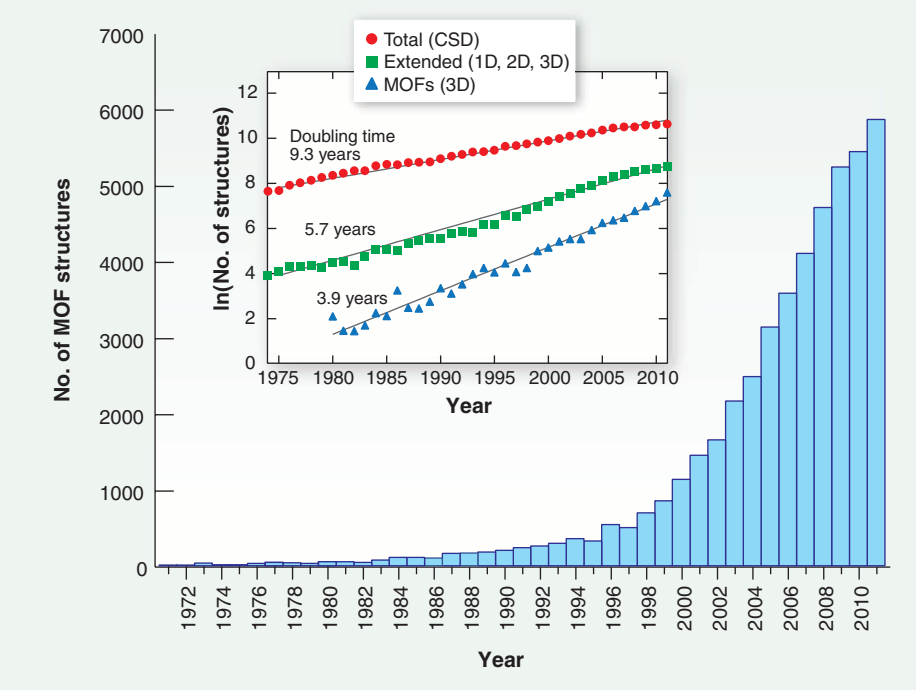


**Fig. 1. Metal-organic framework structures (1D, 2D, and 3D) reported in the Cambridge Structural Database (CSD) from 1971 to 2011.** The trend shows a striking increase during this period for all structure types. In particular, the doubling time for the number of 3D MOFs (inset) is the highest among all reported metal-organic structures.

[1]Department of Chemistry, University of California, Berkeley, CA 94720, USA. [2]Materials Sciences Division, Lawrence Berkeley National Laboratory, Berkeley, CA 94720, USA. [3]Department of Chemistry, Arizona State University, Tempe, AZ 87240, USA. [4]NanoCentury KAIST Institute and Graduate School of Energy, Environment, Water, and Sustainability (World Class University), Daejeon 305-701, Republic of Korea.

*Corresponding author. E-mail: yaghi@berkeley.edu

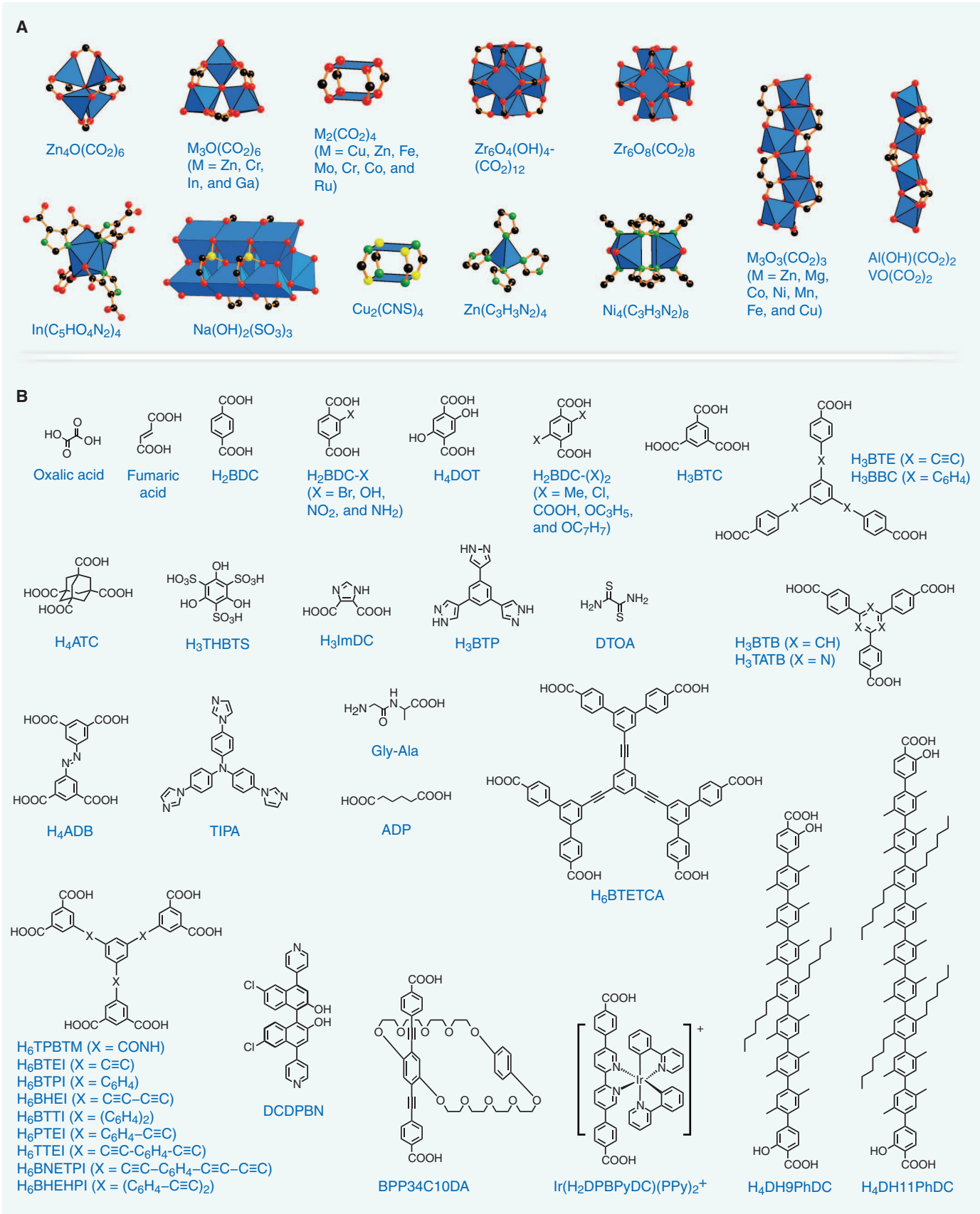


**Fig. 2. Inorganic secondary building units (A) and organic linkers (B) referred to in the text.** Color code: black, C; red, O; green, N; yellow, S; purple, P; light green, Cl; blue polyhedra, metal ions. Hydrogen atoms are omitted for clarity. AIPA, tris(4-(1*H*-imidazol-1-yl)phenyl)amine; ADP, adipic acid; $TTFTB4^-$, 4,4′,4″,4‴-([2,2′-bis(1,3-dithiolylidene)]-4,4′,5,5′-tetrayl)tetrabenzoate.

permanently porous, as is the case for zeolites. The porosity of these compounds was investigated in the 1990s by forcing gas molecules into the crevices at high pressure (*11*). However, proof of permanent porosity requires measurement of reversible gas sorption isotherms at low pressures and temperatures. Nonetheless, as we remarked at that time (*12*), it was then commonplace to refer to materials as "porous" and "open framework" even though such proof was lacking. The first proof of permanent porosity of MOFs was obtained by measurement of nitrogen and carbon dioxide isotherms on layered zinc terephthalate MOF (*12*).

A major advance in the chemistry of MOFs came in 1999 when the synthesis, x-ray single-crystal structure determination, and low-temperature, low-pressure gas sorption properties were reported for the first robust and highly porous MOF, MOF-5 (*13*). This archetype solid comprises $Zn_4O(CO_2)_6$ octahedral SBUs each linked by six chelating 1,4-benzenedicarboxylate ($BDC^{2-}$) units to give a cubic framework (Fig. 2, figs. S2 and S3, and tables S1 and S2). The architectural robustness of MOF-5 allowed for gas sorption measurements, which revealed 61% porosity and a Brunauer-Emmett-Teller (BET) surface area of 2320 $m^2/g$ (2900 $m^2/g$ Langmuir). These values are substantially higher than those commonly found for zeolites and activated carbon (*14*).

To prepare MOFs with even higher surface area (ultrahigh porosity) requires an increase in storage space per weight of the material. Longer organic linkers provide larger storage space and a greater number of adsorption sites within a given material. However, the large space within the crystal framework makes it prone to form interpenetrating structures (two or more frameworks grow and mutually intertwine together). The most effective way to prevent interpenetration is by making MOFs whose topology inhibits interpenetration because it would require the second framework to have a different topology (*15*). Additionally, it is important to keep the pore diameter in the micropore range (below 2 nm) by judicious selection of organic linkers in order to maximize the BET surface area of the framework, because it is known that BET surface areas obtained from isotherms are similar to the geometric surface areas derived from the crystal structure (*16*). In 2004, MOF-177 [$Zn_4O(BTB)_2$; BTB = 4,4′,4″-benzene-1,3,5-triyl-tribenzoate] was reported with the highest surface area at that time (BET surface area = 3780 $m^2/g$, porosity = 83%; Figs. 3A and 4) (*15*), which satisfies the above requirements. In 2010, the surface area was doubled by MOF-200 and MOF-210 [$Zn_4O(BBC)_2$ and $(Zn_4O)_3(BTE)_4(BPDC)_3$, respectively; $BBC^{3-}$ = 4,4′,4″-(benzene-1,3,5-triyl-tris(benzene-4,1-diyl))tribenzoate; BTE = 4,4′,4″-(benzene-1,3,5-triyl-tris(ethyne-2,1-diyl)) tribenzoate; BPDC = biphenyl-4,4′-dicarboxylate] to produce ultrahigh surface areas (4530 $m^2/g$ and 6240 $m^2/g$, respectively) and porosities (90% and 89%) (*17*).

An x-ray diffraction study performed on a single crystal of MOF-5 dosed with nitrogen or argon gas identified the adsorption sites within the pores (*18*). The zinc oxide SBU, the faces, and, surprisingly, the edges of the $BDC^{2-}$ linker serve as adsorption sites. This study uncovered the origin of the high porosity and has enabled the design of MOFs with even higher porosities (Fig. 4 and table S3). Moreover, it has been reported that expanded tritopic linkers based on alkyne rather than phenylene units should increase the number of adsorption sites and increase the surface area (*19*). NU-110 [$Cu_3$(BHEHPI); $BHEHPI^{6-}$ = 5,5′,5″-((((benzene-1,3,5-triyltris(benzene-4,1-diyl)) tris(ethyne-2,1-diyl))-tris(benzene-4,1-diyl)) tris(ethyne-2,1-diyl))triisophthalate], whose organic linker is replete with such edges, displayed a surface area of 7140 $m^2/g$ (Table 1) (*7*, *17*, *20*–*32*).

For many practical purposes, such as storing gases, calculating the surface area per volume is more relevant. By this standard, the value for MOF-5, 2200 $m^2/cm^3$, is among the very best reported for MOFs (for comparison, the value for NU-110 is 1600 $m^2/cm^3$). Note that the external surface area of a nanocube with edges measuring 3 nm would be 2000 $m^2/cm^3$. However, nanocrystallites on this scale with "clean" surfaces would immediately aggregate, ultimately leaving their potential high surface area inaccessible.

### Expansion of Structures by a Factor of 2 to 17

A family of 16 cubic MOFs—IRMOF-1 [also known as MOF-5, which is the parent MOF of the isoreticular (IR) series] to IRMOF-16—with the same underlying topology (isoreticular) was made with expanded and variously functionalized organic linkers (figs. S2 and S3) (*1*, *5*). This development heralded the potential for expanding and functionalizing MOFs for applications in gas storage and separations. The same work demonstrated that a large number of topologically identical but functionally distinctive structures can be made. Note that the topology of these isoreticular MOFs is typically represented with a three-letter code, **pcu**, which refers to its primitive cubic net (*33*). One of the smallest isoreticular structures of MOF-5 is $Zn_4O$(fumarate)$_3$ (*34*); one of the largest is IRMOF-16 [$Zn_4O(TPDC)_3$; $TPDC^{2-}$ = terphenyl-4,4″-dicarboxylate] (*5*) (fig. S2). In this expansion, the unit cell edge is doubled and its volume is increased by a factor of 8. The degree of interpenetration, and thus the porosity and density of these materials, can be controlled by changing the concentration of reactants, temperature, or other experimental conditions (*5*).

The concept of the isoreticular expansion is not simply limited to cubic (**pcu**) structures, as illustrated by the expansion of MOF-177 to give MOF-180 [$Zn_4O(BTE)_2$] and MOF-200, which use larger triangular organic linkers (**qom** net; Fig. 3A and fig. S4) (*15*, *17*). Contrary to the MOF-5 type of expanded framework, expanded structures of MOF-177 are noninterpenetrating despite the high porosity of these MOFs (89% and 90% for MOF-180 and MOF-200, respectively). These results highlight the critical role of selecting topology.

Another MOF of interest is known as HKUST-1 [$Cu_3(BTC)_2$; $BTC^{3-}$ = benzene-1,3,5-tricarboxylate] (*35*); it is composed of Cu paddlewheel [$Cu_2(CO_2)_4$] SBUs (Fig. 2A) and a tritopic organic linker, $BTC^{3-}$. Several isoreticular structures have been made by expansion with $TATB^{3-}$ [4,4′,4″-(1,3,5-triazine-2,4,6-triyl)tribenzoate], $TATAB^{3-}$ [4,4′,4″-((1,3,5-triazine-2,4,6-triyl)tris(azanediyl))tribenzoate], $TTCA^{3-}$ [triphenylene-2,6,10-tricarboxylate], $HTB^{3-}$ [4,4′,4″-(1,3,3a$^1$,4,6,7,9-heptaazaphenalene-2,5,8-triyl)tribenzoate], and $BBC^{3-}$ linkers (**tbo** net; Fig. 3B, fig. S1 and S5, and tables S1 and S2) (*21*, *36*–*39*). The cell volume for the largest reported member [MOF-399, $Cu_3(BBC)_2$] is 17.4 times that of HKUST-1. MOF-399 has the highest void fraction (94%) and lowest density (0.126 $g/cm^3$) of any MOF reported to date (*21*).

Cu paddlewheel units are also combined with various lengths of hexatopic linkers to form another isoreticular series. The first example of one of these MOFs is $Zn_3$(TPBTM) [$TPBTM^{6-}$ = 5,5′,5″-((benzene-1,3,5-tricarbonyl)tris(azanediyl)) triisophthalate], which has a **ntt** net (*40*). Shortly after this report, several isoreticular MOF structures were synthesized (Fig. 3C and fig. S6) (*19*, *20*, *24*, *41*–*48*): $Cu_3$(TPBTM), $Cu_3$(TDPAT), NOTT-112 [$Cu_3$(BTPI)], NOTT-116 [also known as PCN-68; $Cu_3$(PTEI)], PCN-61 [$Cu_3$(BTEI)], PCN-66 [$Cu_3$(NTEI)], PCN-69 [also known as NOTT-119; $Cu_3$(BTTI)], PCN-610 [also known as NU-100; $Cu_3$(TTEI)], NU-108 [$Cu_3$(BTETCA)], NU-109 [$Cu_3$(BNETPI)], NU-110, and NU-111 [$Cu_3$(BHEI)] $TDPAT^{6-}$ = 5,5′,5″-((1,3,5-triazine-2,4,6-triyl)tris(azanediyl))triisophthalate; $BTPI^{6-}$ = 5,5′,5″-(benzene-1,3,5-triyl-tris(benzene-4,1-diyl)) triisophthalate; $PTEI^{6-}$ = 5,5′,5″-((benzene-1,3,5-triyl-tris(benzene-4,1-diyl))tris(ethyne-2,1-diyl)) triisophthalate; $BTEI^{6-}$ = 5,5′,5″-(benzene-1,3,5-triyl-tris(ethyne-2,1-diyl))triisophthalate; $NTEI^{6-}$ = 5,5′,5″-((nitrilotris(benzene-4,1-diyl))tris(ethyne-2,1-diyl))triisophthalate; $BTTI^{6-}$ = 5,5′,5″-(benzene-1,3,5-triyl-tris(biphenyl-4,4′-diyl)) triisophthalate; $TTEI^{6-}$ = 5,5′,5″-(((benzene-1,3,5-triyl-tris(ethyne-2,1-diyl))tris(benzene-4,1-diyl))tris(ethyne-2,1-diyl))triisophthalate; $BTETCA^{6-}$ = 5′,5″″,5‴‴′-(benzene-1,3,5-triyl-tris (ethyne-2,1-diyl))tris(([1,1′:3′,1″-terphenyl]-4,4″-dicarboxylate)); $BNETPI^{6-}$ = 5,5′,5″-(((benzene-1,3,5-triyl-tris(ethyne-2,1-diyl))tris(benzene-4,1-diyl)) tris(buta-1,3-diyne-4,1-diyl))triisophthalate; $BHEI^{6-}$ = 5,5′,5″-(benzene-1,3,5-triyl-tris(buta-1,3-diyne-4,1-diyl))triisophthalate]. Isoreticular materials are not necessarily expansions of the original parent MOF, as exemplified by NU-108, because the **ntt** family has a linker ($BTETCA^{6-}$) with two branching points and two kinds of links (figs. S1B and S7).

A wide variety of metal ions form metal-carboxylate units, and isostructural MOFs can be synthesized by replacing the metal ions in the inorganic SBUs. Indeed, after the appearance of HKUST-1 [$Cu_3(BTC)_2$], an isostructural series of HKUST-1 [$M_3(BTC)_2$, where M = Zn(II), Fe(II), Mo(II), Cr(II), Ru(II)] was prepared by several groups (fig. S5) (*49*–*53*). In the same way as

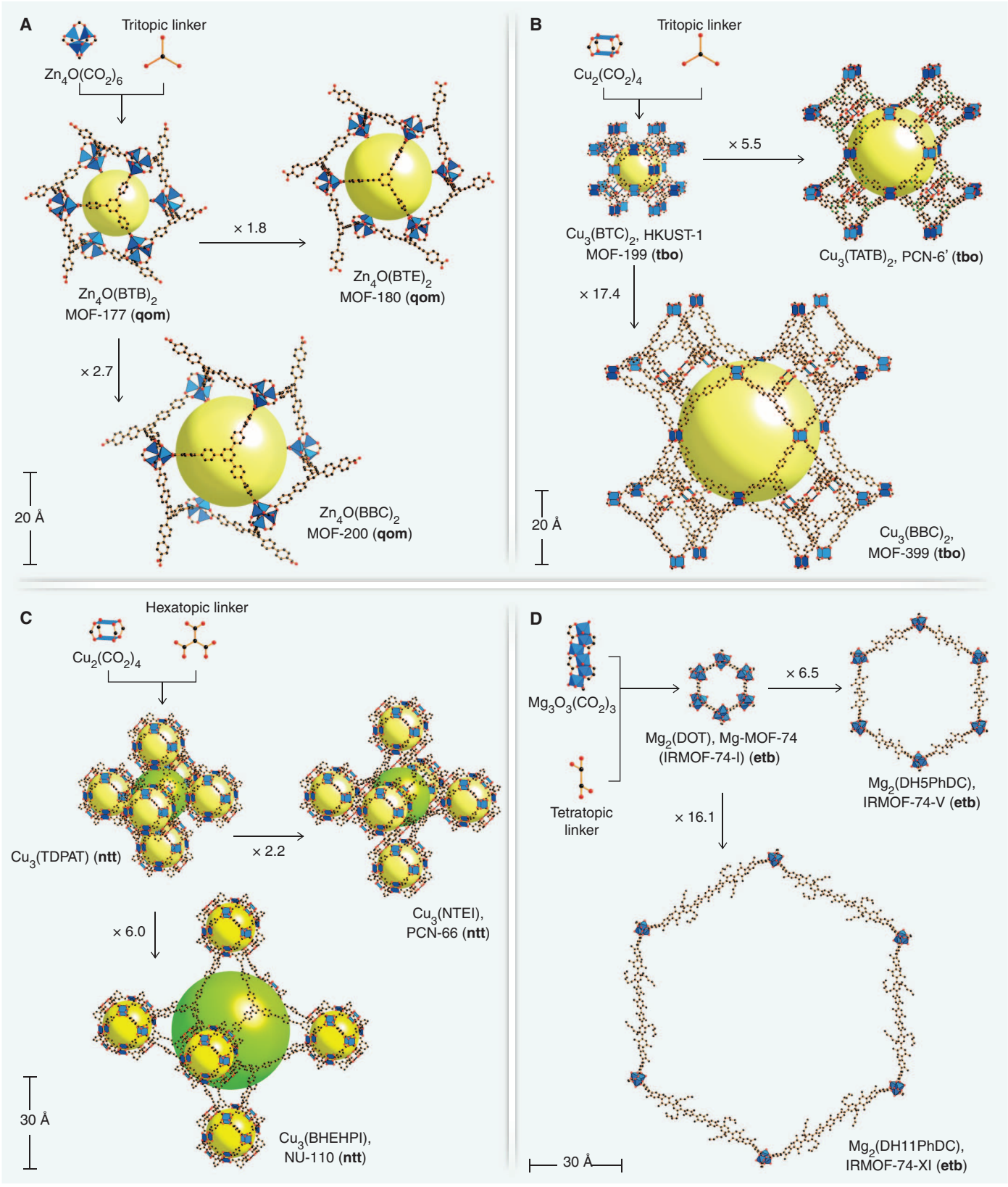


**Fig. 3. Isoreticular expansion of metal-organic frameworks with qom, tbo, ntt, and etb nets.** (**A** to **D**) The isoreticular (maintaining same topology) expansion of archetypical metal-organic frameworks resulting from discrete [(A), (B), and (C)] and rod inorganic SBUs (D) combined with tri-, hexa-, and tetratopic organic linkers to obtain MOFs in **qom** (A), **tbo** (B), **ntt** (C), and **etb** (D) nets, respectively. Each panel shows a scaled comparison of the smallest, medium, and largest crystalline structures of MOFs representative of these nets. The large yellow and green spheres represent the largest sphere that would occupy the cavity. Numbers above each arrow represent the degree of volume expansion from the smallest framework. Color code is same as in Fig. 2; hydrogen atoms are omitted for clarity.

discrete inorganic SBUs, the infinite inorganic rod-type SBUs were also used to synthesize isostructural MOF-74 [$Zn_2$(DOT); DOT = dioxidoterephthalate] (*54*) using divalent metal ions such as Mg, Co, Ni, and Mn (fig. S8) (*55*).

### Exceptionally Large Pore Apertures

Pore openings of MOFs are typically large enough (up to 2 nm) to accommodate small molecules, but rarely are they of appropriate size to permit inclusion of large molecules such as proteins. The best way to increase pore apertures is to use infinite rod-shaped SBUs with linkers of arbitrary length providing periodicity in the other two dimensions, which does not allow for interpenetrating structures. This strategy was implemented by expanding the original phenylene unit of MOF-74 [$M_2$(DOT); $M^{2+}$ = Zn, Mg] structure (*54*) to 2, 3, 4, 5, 6, 7, 9, and 11 phenylene units [DH2PhDC$^{4-}$ to DH11PhDC$^{4-}$, respectively; Fig. 2B, Fig. 3D, and figs. S1B and S8] (*22*). Crystal structures revealed that pore apertures for this series of MOF-74 structures (termed IRMOF-74-I to IRMOF-74-XI) ranged from 14 to 98 Å. The presence of the large pore apertures was also confirmed by transmission electron microscopy (TEM) and scanning electron microscopy (SEM) observation as well as argon adsorption measurements of the guest-free materials. As expected, the pore aperture of IRMOF-74-IX is of sufficient size to allow for green fluorescent protein (barrel structure with diameter of 34 Å and length of 45 Å) to pass into the pores without unfolding. More important, the large pore aperture is of benefit to the surface modification of the pores with various functionalities without sacrificing the porosity (*22*). An oligoethylene glycol–functionalized IRMOF-74-VII [$Mg_2$(DH7PhDC-oeg)] allows inclusion of myoglobin, whereas IRMOF-74-VII with hydrophobic hexyl chains showed a negligible amount of inclusion.

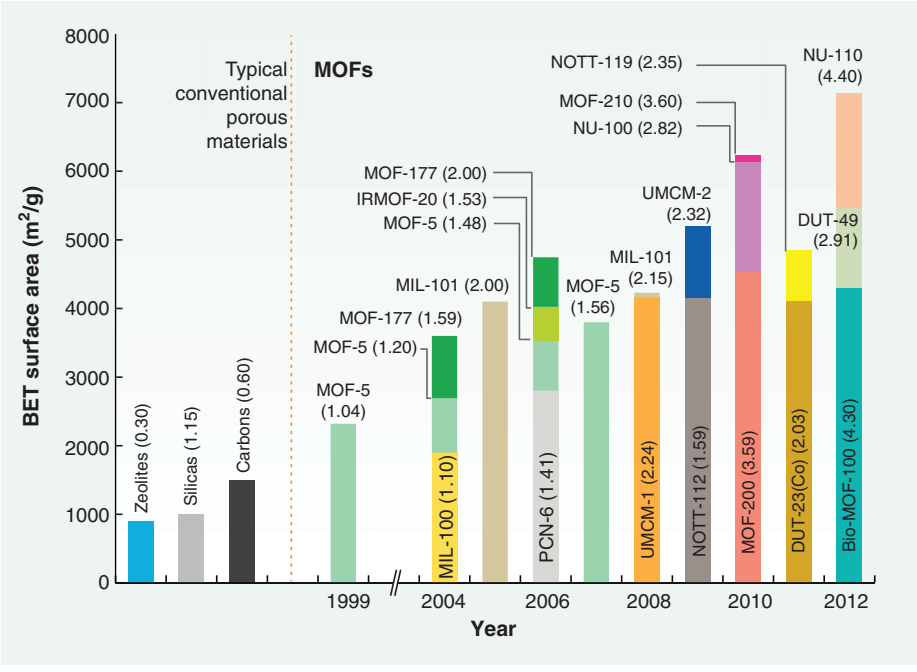


**Fig. 4. Progress in the synthesis of ultrahigh-porosity MOFs.** BET surface areas of MOFs and typical conventional materials were estimated from gas adsorption measurements. The values in parentheses represent the pore volume ($cm^3/g$) of these materials.

### High Thermal and Chemical Stability

Because MOFs are composed entirely of strong bonds (e.g., C-C, C-H, C-O, and M-O), they show high thermal stability ranging from 250° to 500°C (*5*, *56*–*58*). It has been a challenge to make chemically stable MOFs because of their susceptibility to link-displacement reactions when treated with solvents over extended periods of time (days). The first example of a MOF with exceptional chemical stability is zeolitic imidazolate framework–8 [ZIF-8, $Zn(MIm)_2$; $MIm^-$ = 2-methylimidazolate], which was reported in 2006 (*56*). ZIF-8 is unaltered after immersion in boiling methanol, benzene, and water for up to 7 days, and in concentrated sodium hydroxide at 100°C for 24 hours.

**Table 1. Typical properties and applications of metal-organic frameworks.** Metal-organic frameworks exhibiting the lowest and highest values for the indicated property, and those reported first for selected applications, are shown.

| Property or application | Compound | Achieved value or year of report | Reference |
|---|---|---|---|
| *Lowest reported value* | | | |
| Density | MOF-399 | 0.126 $g/cm^3$ | (*21*) |
| *Highest reported value* | | | |
| Pore aperture | IRMOF-74-XI | 98 Å | (*22*) |
| Number of organic linkers | MTV-MOF-5 | 8 | (*7*) |
| Degrees of interpenetration | $Ag_6(OH)_2(H_2O)_4(TIPA)_5$ | 54 | (*23*) |
| BET surface area | NU-110 | 7140 $m^2/g$ | (*20*) |
| Pore volume | NU-110 | 4.40 $cm^3/g$ | (*20*) |
| Excess hydrogen uptake (77 K, 56 bar) | NU-100 | 9.0 wt% | (*24*) |
| Excess methane uptake (290 K, 35 bar) | PCN-14 | 212 mg/g | (*25*) |
| Excess carbon dioxide uptake (298 K, 50 bar) | MOF-200 | 2347 mg/g | (*17*) |
| Proton conductivity (98% relative humidity, 25°C) | $(NH_4)_2(ADP)[Zn_2(oxalate)_3]\cdot 3H_2O$ | $8 \times 10^{-3}$ S/cm | (*26*) |
| Charge mobility | $Zn_2$(TTFTB) | 0.2 $cm^2/V\cdot s$ | (*27*) |
| Lithium storage capacity (after 60 cycles) | $Zn_3(HCOO)_6$ | 560 mAh/g | (*28*) |
| *Earliest report* | | | |
| Catalysis by a MOF | $Cd(BPy)_2(NO_3)_2$ | 1994 | (*29*) |
| Gas adsorption isotherm and permanent porosity | MOF-2 | 1998 | (*12*) |
| Asymmetric catalysis with a homochiral MOF | POST-1 | 2000 | (*31*) |
| Production of open metal site | MOF-11 | 2000 | (*30*) |
| PSM on the organic linker | POST-1 | 2000 | (*31*) |
| Use of a MOF for magnetic resonance imaging | MOF-73 | 2008 | (*32*) |

MOFs based on the Zr(IV) cuboctahedral SBU (Fig. 2A) also show high chemical stability; UiO-66 [$Zr_6O_4(OH)_4(BDC)_6$] and its $NO_2$- and Br-functionalized derivatives demonstrated high acid (HCl, pH = 1) and base resistance (NaOH, pH = 14) (*57*, *58*). The stability also remains when tetratopic organic linkers are used; both MOF-525 [$Zr_6O_4(OH)_4(TpCPP\text{-}H_2)_3$; TpCPP = tetra-*para*-carboxyphenylporphyrin] and 545 [$Zr_6O_8(TpCPP\text{-}H_2)_2$] are chemically stable in methanol, water, and acidic conditions for 12 hours (*59*). Furthermore, a pyrazolate-bridged MOF [$Ni_3(BTP)_2$; $BTP^{3-}$ = 4,4′,4″-(benzene-1,3,5-triyl)tris(pyrazol-1-ide)] is stable for 2 weeks in a wide range of aqueous solutions (pH = 2 to 14) at 100°C (*60*). The high chemical stability observed in these MOFs is expected to enhance their performance in the capture of carbon dioxide from humid flue gas and extend MOFs' applications to water-containing processes.

### Postsynthetic Modification (PSM): Crystals as Molecules

The first very simple, but far from trivial, example of PSM was with the Cu paddlewheel carboxylate MOF-11 [$Cu_2(ATC)$; $ATC^{4-}$ = adamantane-1,3,5,7-tetracarboxylate] (*30*). As-prepared Cu atoms are bonded to four carboxylate O atoms, and the coordination shell is completed typically with coordinated water (Fig. 2A). Subsequent removal of the water from the immobilized Cu atom leaves a coordinatively unsaturated site ("open metal site"). Many other MOFs with such sites have now been generated and have proved to be exceptionally favorable for selective gas uptake and catalysis (*61*–*63*).

The first demonstration of PSM on the organic link of a MOF was reported in 2000 for a homochiral MOF, POST-1 [$Zn_3(\mu_3\text{-}O)(D\text{-}PTT)_6$; $D\text{-}PTT^-$ = (4*S*,5*S*)-2,2-dimethyl-5-(pyridin-4-ylcarbamoyl)-1,3-dioxolane-4-carboxylate] (*31*). It involved *N*-alkylation of dangling pyridyl functionalities with iodomethane and 1-iodohexane to produce *N*-alkylated pyridinium ions exposed to the pore cavity.

More recently, PSM was applied to the dangling amine group of IRMOF-3 [$Zn_4O(BDC\text{-}NH_2)_3$] crystals (*6*). The MOF was submerged in a dichloromethane solution containing acetic anhydride to give the amide derivative in >80% yield. Since then, a large library of organic reactions have been used to covalently functionalize MOF backbones (table S4) (*64*, *65*).

UMCM-1-$NH_2$ [$(Zn_4O)_3(BDC\text{-}NH_2)_3(BTB)_4$] was also acylated with benzoic anhydride to produce the corresponding amide functionality within the pores (*66*). The structures of both IRMOF-3 and UMCM-1-$NH_2$ after modification showed increased hydrogen uptake relative to the parent MOFs, even though there was a reduction in overall surface area (*66*). PSM has also been used to dangle catalytically active centers within the pores. In an example reported in 2005, a Cd-based MOF built from 6,6′-dichloro-4,4′-di(pyridin-4-yl)-[1,1′-binaphthalene]-2,2′-diol (DCDPBN), [$CdCl_2(DCDPBN)$], used orthogonal dihydroxy functionalities to coordinate titanium isopropoxide [$Ti(O^iPr)_4$], thus yielding a highly active, enantioselective asymmetric Lewis acid catalyst (*67*). UMCM-1-$NH_2$ was also functionalized in such a manner to incorporate salicylate chelating groups, which were subsequently metallated with Fe(III) and used as a catalyst for Mukaiyama aldol reactions over multiple catalytic cycles without loss of activity or crystallinity (*68*). Indeed, the remarkable retention of MOF crystallinity and porosity after undergoing the transformation reactions clearly demonstrates the use of MOF crystals as molecules (*69*).

### Catalytic Transformations Within the Pores

The high surface areas, tunable pore metrics, and high density of active sites within the very open structures of MOFs offer many advantages to their use in catalysis (table S5). MOFs can be used to support homogeneous catalysts, stabilize short-lived catalysts, perform size selectivity, and encapsulate catalysts within their pores (*70*). The first example of catalysis in an extended framework, reported in 1994, involved the cyanosilylation of aldehydes in a Cd-based framework [$Cd(BPy)_2(NO_3)_2$; BPy = 4,4′-bipyridine] as a result of axial ligand removal (*29*). This study also highlighted the benefits of MOFs as size-selective catalysts by excluding large substrates from the pores.

In 2006, it was shown that removal of solvent from HKUST-1 exposes open metal sites that may act as Lewis acid catalysts (*71*). MIL-101 [$Cr_3X(H_2O)_2O(BDC)_3$; X = F, OH] and Mn-BTT {$Mn_3[(Mn_4Cl)_3(BTT)_8]_2$; $BTT^{3-}$ = 5,5′,5″-(benzene-1,3,5-triyl)tris(tetrazol-2-ide)} have also been identified as Lewis acid catalysts in which the metal oxide unit functions as the catalytic site upon ligand removal (*62*, *72*). In addition, alkane oxidation, alkene oxidation, and oxidative coupling reactions have also been reported; they all rely on the metal sites within the SBUs for catalytic activity (*73*–*75*). The study of methane oxidation in vanadium-based MOF-48 {$VO[BDC\text{-}(Me)_2]$; Me = methyl} is promising because the catalytic turnover and yield for this oxidation far exceed those of the analogous homogeneous catalysts (*73*).

One early example of the use of a MOF as a heterogeneous catalyst is PIZA-3 [$Mn_2(TpCPP)_2Mn_3$], which contains a metalloporphyrin as part of the framework (*76*). PIZA-3 is capable of hydroxylating alkanes and catalyzes the epoxidation of olefins. Schiff-base and binaphthyl metal complexes have also been incorporated into MOFs to achieve olefin epoxidation and diethyl zinc ($ZnEt_2$) additions to aromatic aldehydes, respectively (*67*, *77*).

The incorporation of porphyrin units within the pores of MOFs can be accomplished during the synthesis (a "ship-in-a-bottle" approach that captures the units as the pores form), as illustrated for the zeolite-like MOF *rho*-ZMOF [$In(HImDC)_2{\cdot}X$; $HImDC^{2-}$ = imidazoledicarboxylate, $X^-$ = counteranion] (*78*). The pores of this framework accommodate high porphyrin loadings, and the pore aperture is small enough to prevent porphyrin from leaching out of the MOF. The porphyrin metal sites were subsequently metallated and used for the oxidation of cyclohexane. The same approach has been applied to several other systems in which polyoxometalates are encapsulated within MIL-101(Cr) and HKUST-1 for applications in the oxidation of alkenes and the hydrolysis of esters in excess water (*79*, *80*).

Integration of nanoparticles for catalysis by PSM has been carried out to enhance particle stability or to produce uniform size distributions. Palladium nanoparticles were incorporated within MIL-101(Cr) for cross-coupling reactions (*81*, *82*). Most recently, a bifunctional catalytic MOF {$Zr_6O_4(OH)_4[Ir(DPBPyDC)(PPy)_2{\cdot}X]_6$; $DPBPyDC^{2-}$ = 4,4′-([2,2′-bipyridine]-5,5′-diyl)dibenzoate, PPy = 2-phenylpyridine} capable of water-splitting reactions was reported (*83*). This MOF uses the organic linker and an encapsulated nanoparticle to transfer an electron to a proton in solution, leading to hydrogen evolution.

### Gas Adsorption for Alternative Fuels and Separations for Clean Air

Much attention is being paid to increasing the storage of fuel gases such as hydrogen and methane under practical conditions. The first study of hydrogen adsorption was reported in 2003 for MOF-5 (*84*). This study confirmed the potential of MOFs for application to hydrogen adsorption, which has led to the reporting of hydrogen adsorption data for hundreds of MOFs (*85*). In general, the functionality of organic linkers has little influence on hydrogen adsorption (*86*), whereas increasing the pore volume and surface area of MOFs markedly enhances the gravimetric hydrogen uptake at 77 K and high pressure, as exemplified by the low-density materials: NU-100 and MOF-210 exhibit hydrogen adsorption as high as 7.9 to 9.0 weight percent (wt%) at 56 bar for both MOFs and 15 wt% at 80 bar for MOF-210 (*17*, *24*). However, increasing the surface area is not always an effective tool for increasing the volumetric hydrogen adsorption, which can be accomplished by increasing the adsorption enthalpy of hydrogen ($Q_{st}$) (*87*). In this context, open metal sites have been suggested and used to enhance the hydrogen uptake capacity and to improve $Q_{st}$ (*61*, *85*). Two MOFs with this characteristic, $Zn_3(BDC)_3[Cu(Pyen)]$ [$Pyen^{2-}$ = 5,5′-((1*E*,1′*E*)-(ethane-1,2-diyl-bis(azanylylidene))bis(methanylylidene))bis(3-methylpyridin-4-ol)] and Ni-MOF-74, have the highest reported initial $Q_{st}$ values: 15.1 kJ/mol and 12.9 kJ/mol, respectively (*58*, *88*). Metal impregnation has also been suggested by computation as a method for increasing the $Q_{st}$ values (*89*). Experiments along these lines show that doping MOFs with alkali metal cations yields only modest enhancements in the total hydrogen uptake and $Q_{st}$ values (*90*, *91*). Although some challenges remain in meeting the U.S. Department of Energy (DOE) system targets (5.5 wt% and 40 g/liter at –40° to 60°C below 100 bar) for hydrogen adsorption (*85*), Mercedes-Benz has already deployed MOF hydrogen fuel tanks in a

fuel cell–powered demonstration model, the F125 (*92*).

An alternative high-density fuel source to hydrogen and gasoline is natural gas (methane). The first study of high-pressure methane adsorption in an extended metal-organic structure was reported in 2000 for $CuSiF_6(BPy)_2$ (*93*), which demonstrated an uptake capacity of 104 mg/g at 36 atm and 298 K. As is the case for hydrogen adsorption, the total gravimetric methane uptake capacity is generally proportional to the pore volume of MOFs. The calculated total uptake values for MOF-177, MOF-200, and MOF-210 are 345 mg/g, 446 mg/g, and 476 mg/g, respectively, at 80 bar and 298 K. These values are much greater than those of any other MOF (*17*). The amount of methane stored in a vessel filled with one of these MOFs is at least double the amount that could be stored in an empty vessel at room temperature and pressures up to 80 bar (*17*). This technology is now being commercialized by BASF for automobile fueling (*94*). The optimal material is not necessarily the one with highest uptake, but rather one that allows minimal uptake at low pressure and highest uptake at higher pressure so as to maximize the working capacity.

MOFs also offer reversible carbon dioxide adsorption and are promising materials for the selective capture of carbon from the atmosphere and flue gas. Carbon dioxide adsorption in MOFs was first reported in 1998 for MOF-2 [Zn(BDC)] (*12*). In 2005, a detailed study of carbon dioxide adsorption in a series of MOFs at room temperature showed MOF-177 to have an uptake capacity of 1470 mg/g at 35 bar (*95*). This uptake of carbon dioxide exceeded that of any known porous material under such conditions. The large quadrupole moment of carbon dioxide molecules causes them to interact with the framework more strongly than hydrogen and methane. As expected, the best excess carbon dioxide uptake reported to date was observed in a MOF with ultrahigh porosity, MOF-200 (2437 mg/g at 50 bar and 298 K) (*17*). In practical terms, a gas tank filled with MOF-177 or MOF-200 would store 9 times or 17 times as much carbon dioxide at 35 bar, respectively, as the corresponding pressurized tank without MOF. On the other hand, many carbon dioxide capture applications will operate at low pressure so that the Henry's law constant (i.e., initial slope of the isotherm) can be used as an indicator of the carbon dioxide selectivity. MOFs with open metal sites were found to have desirable high initial $Q_{st}$ values of 62 kJ/mol and 47 kJ/mol for MIL-101(Cr) and Mg-MOF-74, respectively (*96*, *97*), thereby offering enhanced carbon dioxide uptake and selectivity at low pressures. Basic nitrogen centers have also been post-synthetically added to MOFs with open metal sites by using *N*,*N*′-dimethylethylenediamine (mmen), where the highest initial $Q_{st}$ for $H_3[(Cu_4Cl)_3(BTTri)_8(mmen)_{12}]$ [$BTTri^{3-}$ = 4,4′,4″-(benzene-1,3,5-triyl)tris(1,2,3-triazol-1-ide)] is estimated to be 96 kJ/mol (*98*). Because the ideal material for carbon dioxide capture from flue and combustion gases requires high selectivity in the presence of water, it is useful to target MOFs in which the competition between carbon dioxide and water for adsorption is minimized. In this respect, chemical binding of carbon dioxide in a recent MOF to make organic carbonates reversibly is a promising approach (*99*).

Gas storage experiments on MOFs have also been extended to the separation of hydrocarbons, toxic molecules (e.g., ammonia and chlorine), and water. For instance, $Cu_2(PZDC)_2(Pyz)$ (PZDC = pyrazine-2,3-dicarboxylate; Pyz = pyrazine) selectively takes up acetylene over carbon dioxide through hydrogen bonding between acetylene and oxygen atoms on the MOF internal surface (*100*). Ammonia was previously considered to be too reactive for MOFs; however, chemically stable Zr-MOFs, such as UiO-66-$NH_2$ [$Zr_6O_4(OH)_4(BDC\text{-}NH_2)_6$] and other derivatives, maintain their structures after the process of ammonia adsorption and desorption (*101*).

Gas separation processes in MOFs generally rely on both the size of the pores and the affinity of MOFs for the targeted gases. After the discovery of permanent porosity of MOFs, equilibrium adsorption isotherms for various gases were collected to estimate potential gas selectivity. High selectivity calculated from equilibrium data does not guarantee high selectivity under dynamic gas separation conditions. The latter is desirable in industrial processes, because the diffusion rate and $Q_{st}$ value of gas binding in the adsorbent are sensitive to the operating conditions. One of the earliest examples of a dynamic separation was performed using a gas chromatographic column filled with MOF-508 [$Zn_2(BDC)_2(BPy)$] to separate alkanes such as *n*-pentane, *n*-hexane, 2,2-dimethylbutane, and 2-methylpentane (*102*). Another early example is the removal of tetrahydrothiophene (THT) from methane by means of a fixed bed containing $Cu_3(BTC)_2$ (*3*). The color of the $Cu_3(BTC)_2$ changed from deep blue to light green, indicating that THT was adsorbed to the copper open metal sites. More recently, it has been reported that Mg and Fe-MOF-74, packed in a column, exhibit enhanced carbon dioxide separation from methane and $C_1$ to $C_3$ hydrocarbon, respectively (*61*, *103*).

## Proton Conductivity for Fuel Cell Applications

The use of MOFs as inexpensive proton-conducting membranes for fuel cell applications represents a new direction in MOF research (*104*). The first conductivity measurements were performed on $Cu(DTOA)(HOC_2H_4)_2$, albeit with a relatively low reported conductivity (*105*). It is now understood that any improvement in the water-mediated proton conductivity of MOFs requires the addition of an acid functionality, such as carboxylic, phosphonic, or sulfonic acid, as demonstrated by several functionalized versions of MIL-53 [Fe(OH)(BDC-X); X = H, $NH_2$, OH, $(COOH)_2$] (*106*). This finding is further supported by the demonstrated high proton conductivity—$2.5 \times 10^{-3}$ S/cm at 98% relative humidity and 60°C—of MOFs with highly acidic pores [PCMOF-5, $La(H_5DTP)(H_2O)_3$; $DTP^{8-}$ = 1,2,4,5-tetrakisphosphonomethylbenzene] (*107*). Alternatively, high proton conductivity is also observed in one-dimensional (1D) metal-organic structures lacking any acidic functionality, as in $Fe(oxalate)(H_2O)_2$. Here, coordinated water molecules act as proton donors, with their 1D arrangement within crystals facilitating the rate of proton transport (*108*).

If MOFs are to serve as proton conductors for practical applications, they must be able to function at relatively high operating temperatures (120° to 180°C) and in anhydrous conditions (*109*). A simple strategy that may be used to meet these practical considerations is the impregnation of MOFs with amphoteric molecules such as imidazole. For instance, 1*H*-1,2,4-triazole–loaded PCMOF-2 [$Na_3$(THBTS); $THBTS^{3-}$ = 2,4,6-trihydroxy-1,3,5-benzenetrisulfonate] has a higher conductivity than the MOF without triazole (*110*). Similar results were also obtained for imidazole-doped Al(OH)(NDC) (NDC = 1,4-naphthalenedicarboxylate) (*111*). Even higher conductivity was observed when histamine was used as a proton carrier (*112*). These exciting results indicate that high-mobility proton carriers situated within the pore play a key role in achieving MOFs with high proton conductivity.

Extensive research has been devoted to realizing polymer-supported electrolyte membrane fuel cells consisting of perfluorosulfonic acid polymers (e.g., Nafion); however, these polymers have some drawbacks, such as operation temperature, humidity, and cost (*109*). MOFs will be attractive candidates for this application because of their tunable pore size and functionality as well as their chemical and thermal stability.

## MOF Nanocrystals

The advantages of MOFs are not solely limited to properties that originate from their pore structure and functionalities. By virtue of the diverse synthetic procedures reported, the size and morphology of MOF nanocrystals can be precisely controlled (*113*). Several groups have recently reviewed the preparation of MOF nanocrystals for membrane and thin-film applications (*2*, *114*, *115*).

In 2003, the synthesis of nanocrystalline MOFs was accomplished at room temperature for MOF-5, affording crystal sizes of 70 to 90 nm (*116*). The obtained MOF samples were crystalline and porous but without controlled morphology. It was not until 2009 that precise control of MOF nanocrystal morphology was reported (*117*): rhombic dodecahedral ZIF-8 nanocrystals with an estimated average diameter of 40 nm, narrow size distribution, high crystallinity, porosity, and chemical stability. A follow-up study revealed that the nucleation process in ZIF nanocrystal formation is initially slow, followed by a rapid process of crystal growth (*118*). Interestingly, the study showed that the morphology of the nanocrystals transformed from cubic to rhombic dodecahedra in the last stage of crystal formation. This result indicated that the morphology of nanocrystals can be tuned through the optimization of synthetic conditions. Furthermore, soc-MOF-1

$\{[M_6O_2(ADB)_3(H_2O)_6](H_2O)_6(NO_3)_2$; $ADB^{4-}$ = 3,3′,5,5′-azobenzenetetracarboxylate; M = In(III), Ga(III)} and HKUST-1 nanocrystals have adopted several morphologies with their respective diameters in the submicrometer to micrometer range (*119*, *120*).

The assembly of MOF nanocrystals is of particular interest in MOF research because organized nanostructures comprising one or more nanocrystal types may have distinctive properties similar to those seen in metal nanocrystal superlattices (*121*). Only a limited number of examples have been reported to date; however, closely packed 2D superlattice structures of ZIF-8, soc-MOF-1, and UiO-66 were observed by SEM (*119*, *122*, *123*). Applying an ac electric field created linear chain structures of ZIF-8, and the alignment of the nanocrystals was controlled by the anisotropic nature of surface (*124*). Clearly, the synthesis of nanocrystals, their assembly into larger structures, and their incorporation into devices are research areas of increasing interest.

### The Materials Beyond

At present, MOF chemistry has matured to the point where the composition, structure, functionality, porosity, and metrics of a metal-organic structure can be designed for a specific application. This precise control over the assembly of materials is expected to propel this field further into new realms of synthetic chemistry in which far more sophisticated materials may be accessed. For example, materials can be envisaged as having (i) compartments linked together to operate separately, yet function synergistically; (ii) dexterity to carry out parallel operations; (iii) ability to count, sort, and code information (*7*); and (iv) capability of dynamics with high fidelity (*125*, *126*).

To appreciate how such materials may be achieved, it is important to step back and consider the gamut of materials studied thus far. In general, crystalline materials are largely composed of a few building units as constituents of their underlying chemical structure. For example, common solid-state materials such as zeolites, alloys, polymers, and even MOFs and nanocrystals are each constructed from one or two kinds of repeating units (Fig. 5). The same is true for the entire landscape of human-made crystalline materials. This self-similarity of structures is quite unlike the heterogeneity and multiplicity that characterize biological molecules. However, the building of materials from as few as three or four different building units remains an outstanding challenge because such chemistry is believed to give mixed phases rather than a single phase comprising mixed components.

It is our view that vast opportunities exist for making materials from an increasing number of unique building units and that a transformative chemistry is yet to be uncovered for achieving these materials. This new materials space that is expected to emerge from linking multiple kinds of building units will have unlimited possibilities, especially when the building units are arranged in specific sequences within crystals. We propose to call this space "the materials beyond." One can imagine materials with unique sequences of building units that code for specific functions. Materials capable of complex operations and transformations could be used in applications such as conversion of carbon dioxide to fuels, methane to higher alkanes, and water to hydrogen. Once we begin to think in terms of heterogeneity of composition, shape, size, and orientation of building units, there is no limit to the different scenarios for making materials endowed with unusual complexity. Such materials go beyond merely linking building units through strong bonds, as in MOFs.

In 2010, a simple strategy was proposed and demonstrated to introduce further complexity to crystalline structures (Fig. 6A) (*7*). In this work, 18 MTV-MOF-5–type structures were synthesized using variously functionalized $BDC^{2-}$ linkers [$NH_2$, Br, $(Cl)_2$, $NO_2$, $(CH_3)_2$, $C_4H_4$, $(OC_3H_5)_2$, and $(OC_7H_7)_2$]. One of these structures contains eight different functionalities in one phase. The backbone structure (same as MOF-5) is ordered, whereas functional groups incorporated into the framework are varied and disordered. The complex arrangements of these functionalities in the pores can lead to unusual properties; for instance, MTV-MOFs showed improved hydrogen and carbon dioxide uptake capacities relative to MOFs comprising a single organic linker (*7*). This finding clearly demonstrates that MTV-MOFs are not simple linear combinations of their constituents.

Precise control of the functionality arrangement in MOFs is still a looming challenge; however, a new strategy that is widely used for peptide synthesis has been used to systematically control a sequence of functionalities via solid-phase synthesis. Metal-organic complex arrays (MOCAs) are heterometallic complexes in which different metal-organic centers are connected to an amino acid backbone (Fig. 6B) (*127*). The solid-phase synthesis strategy for connecting these units allowed for careful control of the sequence, nuclearity, and length of up to six metal centers including Pt(II), Rh(III), and Ru(II). Potentially MOCAs can serve as functionalities within MOFs to affect sequence-dependent properties. This idea may also manifest itself in materials recently prepared by the sequential deposition of multilayer MOF thin films (*128*).

It is not always necessary to exercise multiple linkers or specific sequences to acquire heterogeneity in MOFs without losing either crystallinity or porosity. Recently, microporous MOF-5 materials in which each crystal contains a system of mesopores and macropores have been synthesized by use of a controlled amount of 4-(dodecyloxy)benzoic acid (DBA) to a reaction

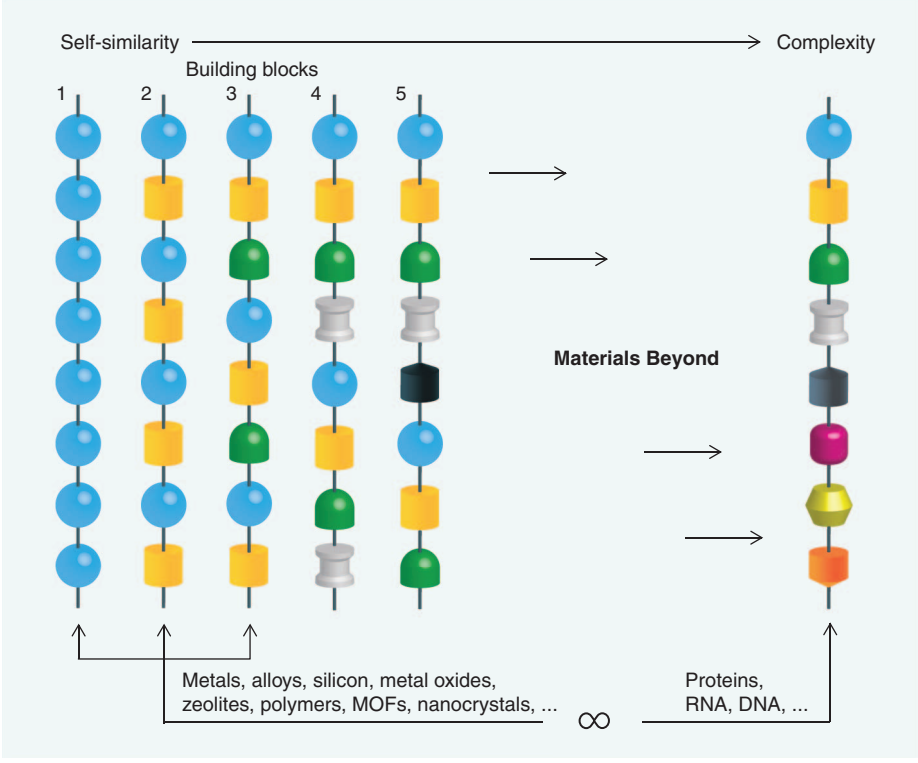


**Fig. 5. Crystalline chemical structures of some of the most useful materials.** These materials (metals, alloys, silicon, metal oxides, zeolites, and polymers) are constructed from few kinds of building units (one to three) to make largely self-similar materials in which such building units repeat periodically throughout the material. Few examples exist of synthetic crystals with more than three building units, as found in biological structures (proteins, RNA, and DNA). The linking of building units by strong bonds (reticular chemistry) as exemplified by the construction of MOFs is useful in developing the structure and function space of the "materials beyond."

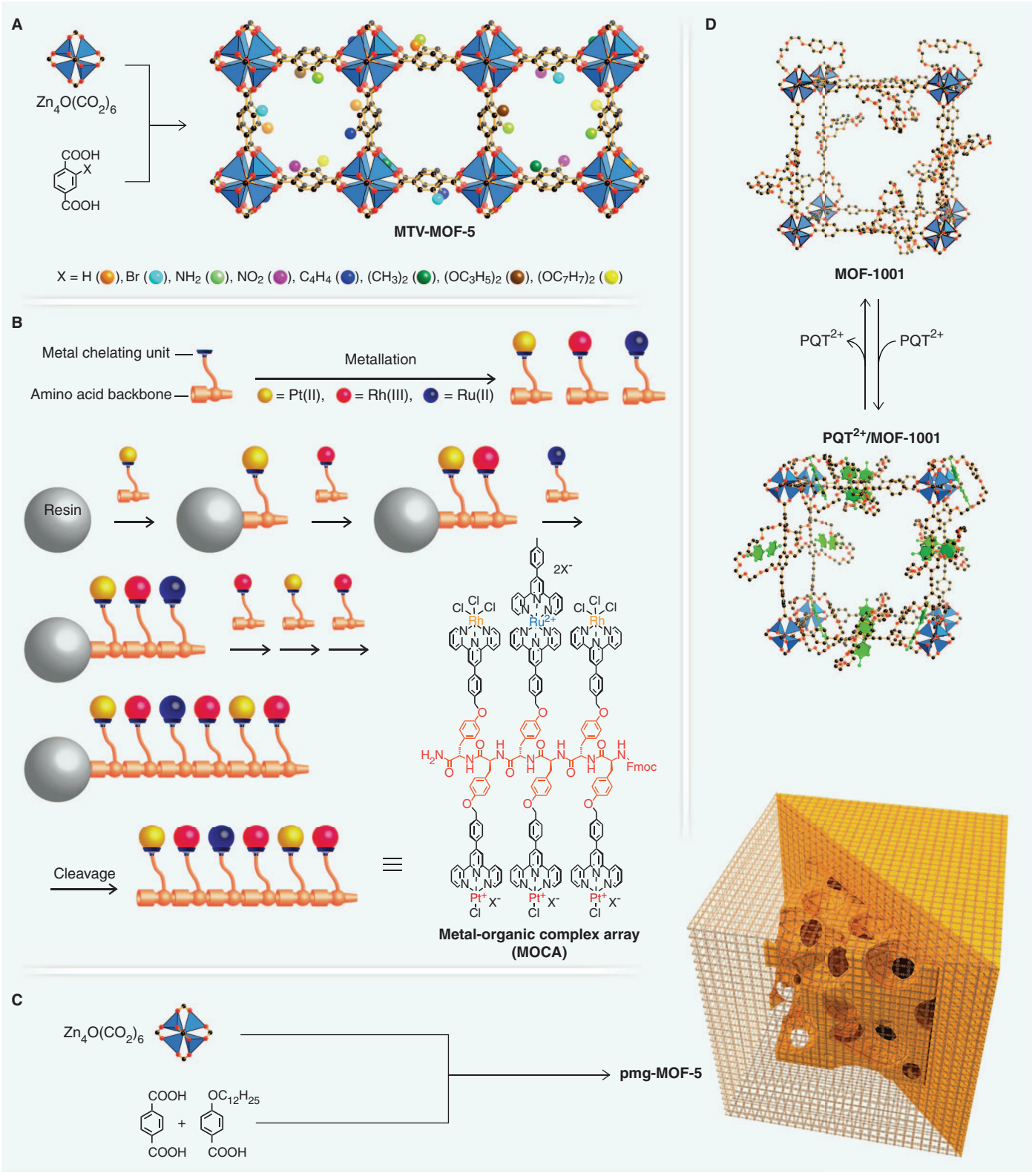


**Fig. 6. Examples of creating heterogeneity within crystalline materials.** (**A**) MTV-MOF-5, in which a heterogeneous mixture of functionalities decorates the interior of the crystals to provide an environment capable of highly selective binding of carbon dioxide. (**B**) Schematic representation of the synthesis of MOCAs, which have a heterogeneity created by arranging metal complexes in specific sequences to give sequence-dependent properties. (**C**) Heterogeneity within order produced in crystals of MOFs (pmg-MOF-5), where mesopores and macropores are encased in microporous MOF-5 to give unusual carbon dioxide capture properties. (**D**) A MOF (MOF-1001) constructed from linkers having polyether rings, which in themselves create stereoelectronically specific binding of substrate paraquat ($PQT^{2+}$). Atom colors are as in Fig. 2; blue polyhedra, Zn. Hydrogen atoms are omitted for clarity.

mixture of MOF-5 (Fig. 6C) (*129*). By addition of DBA, an entirely sponge-like MOF-5 crystal was obtained, whereas mesopores and macropores fully enclosed by a thick microporous MOF-5 sheath (pomegranate-like crystals; pmg-MOF-5) were obtained when a lesser amount of DBA was used. In situ synchrotron powder x-ray diffraction measurements revealed that the mesopores and macropores of pmg-MOF-5 can act as additional carbon dioxide adsorption sites, even though the sponge-like MOF-5 crystals did not show such behavior.

Heterogeneity can also be introduced when multiple metal ions are used in the synthesis of materials termed core-shell structures (*130*). Unlike metal-doped MOFs (*131*), core-shell structures form two compositionally distinct solid phases at their respective interface. Although little is known about the interface of the two phases, film structural analysis of single crystals containing both Zn and Cu domains {$Zn_2(NDC)_2(DABCO)$/$Cu_2(NDC)_2(DABCO)$; DABCO = 1,4-diazabicyclo[2.2.2]octane} reveals that the Cu phase was grown on the surface of the Zn phase with a small in-plane rotation angle (*130*). Precise control of such angles may create interfaces that can be exploited for separation and filtration applications.

MOFs comprising interconnected architectural domains that operate independently are also of high interest. In 2009, a "concept transfer" from the biological world successfully accomplished this goal (*126*). MOF-1001 [$Zn_4O(BPP34C10DA)_3$; $BPP34C10DA^{2-}$ = 4,4′-(2,5,8,11,14,16,19,22,25,28-decaoxa-1,15(1,4)-dibenzenacyclooctacosaphane-$1^2$,$1^5$-diylbis(ethyne-2,1-diyl))dibenzoate] uses periodic crown ether receptors attached to the architectural framework; this endows the pore with active domains capable of molecular recognition of highly disordered guests in a stereoelectronically controlled fashion (Fig. 6D) (*125*). This advancement exploited the mechanism of conformational changes that afford biological macromolecules the capabilities of molecular recognition and installed a new active domain that functions independently of the traditional sorting (i.e., shape and size selectivity of the pore aperture) and coverage domains (i.e., internal pore surface binding). Further evidence for the potential creation of such materials was reported in a MOF [$Zn(Gly\text{-}Ala)_2$; Gly-Ala = glycylalanine] constructed from a flexible dipeptide linker (*132*). This MOF displayed adaptable porosity as a result of the linker, evoking comparisons to the conformational selection that is characteristic of proteins.

MOF architectures reminiscent of Russian dolls composed of nested interconnected cages {cage-within-cage structure; CPM-7 [$Zn_{26}O_3(OH)_4(FDA)_{30}\cdot(H_2O)_{12}(Et_2NH_2)_6$] ($FDA^{2-}$ = furan-2,5-dicarboxylate), CPM-24 [$Co_9(OH)_2(acetate)(BTC)_4(IN)_8\cdot(H_2O)_4(Me_2NH_2)_5$] ($IN^-$ = isonicotinate)} can be another way to introduce irregularity within a single parent structure (*133*, *134*). These nested structures provide exciting potential for the assembly of various connected domains whose internal and external environments can be manipulated to operate independently to suit particular functions (*133*, *134*).

The chemistry and applications of MOFs have progressed substantially since their original inception more than a decade ago. Although it is difficult to rule out the possibility of major advancements arising from MOFs that are compiled from a limited number of building blocks, it is our belief that the future of MOFs lies in the creation of materials whose constituents are many and are systematically varied.

### References and Notes


1. O. M. Yaghi *et al.*, Reticular synthesis and the design of new materials. *Nature* **423**, 705–714 (2003). doi: 10.1038/nature01650; pmid: 12802325
2. 2012 metal-organic frameworks issue. *Chem. Rev.* **112**, 673–1268 (2012); http://pubs.acs.org/toc/chreay/112/2.
3. U. Mueller *et al.*, Metal-organic frameworks—prospective industrial applications. *J. Mater. Chem.* **16**, 626 (2006). doi: 10.1039/b511962f
4. M. Jacoby, Heading to market with MOFs. *Chem. Eng. News* **86**, 13 (2008). doi: 10.1021/cen-v086n034.p013
5. M. Eddaoudi *et al.*, Systematic design of pore size and functionality in isoreticular MOFs and their application in methane storage. *Science* **295**, 469–472 (2002). http://www.ncbi.nlm.nih.gov/entrez/query.fcgi?cmd=Retrieve&db=PubMed&list_uids=11799235&dopt=Abstract. doi: 10.1126/science.1067208; pmid: 11799235
6. Z. Wang, S. M. Cohen, Postsynthetic covalent modification of a neutral metal-organic framework. *J. Am. Chem. Soc.* **129**, 12368–12369 (2007). doi: 10.1021/ja074366o; pmid: 17880219
7. H. Deng *et al.*, Multiple functional groups of varying ratios in metal-organic frameworks. *Science* **327**, 846–850 (2010). doi: 10.1126/science.1181761; pmid: 20150497
8. A. F. Wells, *Structural Inorganic Chemistry* (Oxford Univ. Press, New York, 1984).
9. Y. Kinoshita, I. Matsubara, T. Higuchi, Y. Saito, The crystal structure of bis(adiponitrilo)copper(I) nitrate. *Bull. Chem. Soc. Jpn.* **32**, 1221–1226 (1959). doi: 10.1246/bcsj.32.1221
10. O. M. Yaghi, H. Li, Hydrothermal synthesis of a metal-organic framework containing large rectangular channels. *J. Am. Chem. Soc.* **117**, 10401–10402 (1995). doi: 10.1021/ja00146a033
11. M. Kondo, T. Yoshitomi, H. Matsuzaka, S. Kitagawa, K. Seki, Three-dimensional framework with channeling cavities for small molecules: $[M_2(4,4'\text{-bpy})_3(NO_3)_4]\cdot xH_2O\}_n$ (M = Co, Ni, Zn). *Angew. Chem. Int. Ed. Engl.* **36**, 1725–1727 (1997). doi: 10.1002/anie.199717251
12. H. Li, M. Eddaoudi, T. L. Groy, O. M. Yaghi, Establishing microporosity in open metal-organic frameworks: Gas sorption isotherms for Zn(BDC) (BDC = 1,4-benzenedicarboxylate). *J. Am. Chem. Soc.* **120**, 8571–8572 (1998). doi: 10.1021/ja981669x
13. H. Li, M. Eddaoudi, M. O'Keeffe, O. M. Yaghi, Design and synthesis of an exceptionally stable and highly porous metal-organic framework. *Nature* **402**, 276 (1999). doi: 10.1038/46248
14. H. Furukawa, O. M. Yaghi, Storage of hydrogen, methane, and carbon dioxide in highly porous covalent organic frameworks for clean energy applications. *J. Am. Chem. Soc.* **131**, 8875–8883 (2009). doi: 10.1021/ja9015765; pmid: 19496589
15. H. K. Chae *et al.*, A route to high surface area, porosity and inclusion of large molecules in crystals. *Nature* **427**, 523–527 (2004). doi: 10.1038/nature02311; pmid: 14765190
16. K. S. Walton, R. Q. Snurr, Applicability of the BET method for determining surface areas of microporous metal-organic frameworks. *J. Am. Chem. Soc.* **129**, 8552–8556 (2007). doi: 10.1021/ja071174k; pmid: 17580944
17. H. Furukawa *et al.*, Ultrahigh porosity in metal-organic frameworks. *Science* **329**, 424–428 (2010). http://www.ncbi.nlm.nih.gov/entrez/query.fcgi?cmd=Retrieve&db=PubMed&list_uids=20595583&dopt=Abstract. doi: 10.1126/science.1192160; pmid: 20595583
18. J. L. C. Rowsell, E. C. Spencer, J. Eckert, J. A. K. Howard, O. M. Yaghi, Gas adsorption sites in a large-pore metal-organic framework. *Science* **309**, 1350–1354 (2005). http://www.ncbi.nlm.nih.gov/entrez/query.fcgi?cmd=Retrieve&db=PubMed&list_uids=16123294&dopt=Abstract. doi: 10.1126/science.1113247; pmid: 16123294
19. O. K. Farha *et al.*, Designing higher surface area metal-organic frameworks: Are triple bonds better than phenyls? *J. Am. Chem. Soc.* **134**, 9860–9863 (2012). doi: 10.1021/ja302623w; pmid: 22670563
20. O. K. Farha *et al.*, Metal-organic framework materials with ultrahigh surface areas: Is the sky the limit? *J. Am. Chem. Soc.* **134**, 15016–15021 (2012). doi: 10.1021/ja3055639; pmid: 22906112
21. H. Furukawa *et al.*, Isoreticular expansion of metal-organic frameworks with triangular and square building units and the lowest calculated density for porous crystals. *Inorg. Chem.* **50**, 9147–9152 (2011). doi: 10.1021/ic201376t; pmid: 21842896
22. H. Deng *et al.*, Large-pore apertures in a series of metal-organic frameworks. *Science* **336**, 1018–1023 (2012). doi: 10.1126/science.1220131; pmid: 21728370
23. H. Wu, J. Yang, Z.-M. Su, S. R. Batten, J.-F. Ma, An exceptional 54-fold interpenetrated coordination polymer with $10^3$-srs network topology. *J. Am. Chem. Soc.* **133**, 11406–11409 (2011). doi: 10.1021/ja202303b; pmid: 21728370
24. O. K. Farha *et al.*, De novo synthesis of a metal-organic framework material featuring ultrahigh surface area and gas storage capacities. *Nat. Chem.* **2**, 944–948 (2010). doi: 10.1038/nchem.834; pmid: 20966950
25. S. Ma *et al.*, Metal-organic framework from an anthracene derivative containing nanoscopic cages exhibiting high methane uptake. *J. Am. Chem. Soc.* **130**, 1012–1016 (2008). doi: 10.1021/ja0771639; pmid: 18163628
26. M. Sadakiyo, T. Yamada, H. Kitagawa, Rational designs for highly proton-conductive metal-organic frameworks. *J. Am. Chem. Soc.* **131**, 9906–9907 (2009). doi: 10.1021/ja9040016; pmid: 19621952
27. T. C. Narayan, T. Miyakai, S. Seki, M. Dincă, High charge mobility in a tetrathiafulvalene-based microporous metal-organic framework. *J. Am. Chem. Soc.* **134**, 12932–12935 (2012). doi: 10.1021/ja3059827
28. K. Saravanan, M. Nagarathinam, P. Balaya, J. J. Vittal, Lithium storage in a metal organic framework with diamondoid topology—a case study on metal formates. *J. Mater. Chem.* **20**, 8329 (2010). doi: 10.1039/c0jm01671c
29. M. Fujita, Y. J. Kwon, S. Washizu, K. Ogura, Preparation, clathration ability, and catalysis of a two-dimensional square network material composed of cadmium(II) and 4,4′-bipyridine. *J. Am. Chem. Soc.* **116**, 1151–1152 (1994). doi: 10.1021/ja00082a055
30. B. Chen *et al.*, $Cu_2(ATC)\cdot 6H_2O$: Design of open metal sites in porous metal-organic crystals (ATC: 1,3,5,7-adamantane tetracarboxylate). *J. Am. Chem. Soc.* **122**, 11559–11560 (2000). doi: 10.1021/ja003159k
31. J. S. Seo *et al.*, A homochiral metal-organic porous material for enantioselective separation and catalysis. *Nature* **404**, 982–986 (2000). doi: 10.1038/35010088; pmid: 10801124
32. K. M. L. Taylor, W. J. Rieter, W. Lin, Manganese-based nanoscale metal-organic frameworks for magnetic resonance imaging. *J. Am. Chem. Soc.* **130**, 14358–14359 (2008). doi: 10.1021/ja803777x; pmid: 18844356
33. M. O'Keeffe, M. A. Peskov, S. J. Ramsden, O. M. Yaghi, The Reticular Chemistry Structure Resource (RCSR) database of, and symbols for, crystal nets. *Acc. Chem. Res.* **41**, 1782–1789 (2008). doi: 10.1021/ar800124u; pmid: 18834152
34. M. Xue *et al.*, New prototype isoreticular metal-organic framework $Zn_4O(FMA)_3$ for gas storage. *Inorg. Chem.* **48**, 4649–4651 (2009). doi: 10.1021/ic900486r; pmid: 19405500

35. S. S.-Y. Chui, S. M.-F. Lo, J. P. H. Charmant, A. G. Orpen, I. D. Williams, A chemically functionalizable nanoporous material $[Cu_3(TMA)_2(H_2O)_3]_n$. *Science* **283**, 1148–1150 (1999). doi: 10.1126/science.283.5405.1148; pmid: 10024237
36. X.-S. Wang, S. Ma, D. Sun, S. Parkin, H.-C. Zhou, A mesoporous metal-organic framework with permanent porosity. *J. Am. Chem. Soc.* **128**, 16474–16475 (2006). doi: 10.1021/ja066616r; pmid: 17177376
37. D. Sun, S. Ma, Y. Ke, D. J. Collins, H.-C. Zhou, An interweaving MOF with high hydrogen uptake. *J. Am. Chem. Soc.* **128**, 3896–3897 (2006). doi: 10.1021/ja058777l; pmid: 16551082
38. S. Ma *et al.*, Framework-catenation isomerism in metal-organic frameworks and its impact on hydrogen uptake. *J. Am. Chem. Soc.* **129**, 1858–1859 (2007). doi: 10.1021/ja067435s; pmid: 17256862
39. X.-S. Wang *et al.*, A large-surface-area boracite-network-topology porous MOF constructed from a conjugated ligand exhibiting a high hydrogen uptake capacity. *Inorg. Chem.* **48**, 7519–7521 (2009). doi: 10.1021/ic901073w; pmid: 19606845
40. Y. Zou, M. Park, S. Hong, M. S. Lah, A designed metal-organic framework based on a metal-organic polyhedron. *Chem. Commun.* **2008**, 2340–2342 (2008). doi: 10.1039/b801103f; pmid: 18473063
41. Y. Yan *et al.*, Exceptionally high $H_2$ storage by a metal-organic polyhedral framework. *Chem. Commun.* **2009**, 1025–1027 (2009). doi: 10.1039/b900013e; pmid: 19225624
42. D. Zhao, D. Yuan, D. Sun, H.-C. Zhou, Stabilization of metal-organic frameworks with high surface areas by the incorporation of mesocavities with microwindows. *J. Am. Chem. Soc.* **131**, 9186–9188 (2009). doi: 10.1021/ja901109t; pmid: 19530682
43. D. Yuan, D. Zhao, D. Sun, H.-C. Zhou, An isoreticular series of metal-organic frameworks with dendritic hexacarboxylate ligands and exceptionally high gas-uptake capacity. *Angew. Chem. Int. Ed.* **49**, 5357–5361 (2010). doi: 10.1002/anie.201001009
44. Y. Yan *et al.*, Metal-organic polyhedral frameworks: High $H_2$ adsorption capacities and neutron powder diffraction studies. *J. Am. Chem. Soc.* **132**, 4092–4094 (2010). doi: 10.1021/ja1001407; pmid: 20199070
45. D. Yuan, D. Zhao, H.-C. Zhou, Pressure-responsive curvature change of a "rigid" geodesic ligand in a (3,24)-connected mesoporous metal-organic framework. *Inorg. Chem.* **50**, 10528–10530 (2011). doi: 10.1021/ic201744n; pmid: 21942344
46. B. Zheng, J. Bai, J. Duan, L. Wojtas, M. J. Zaworotko, Enhanced $CO_2$ binding affinity of a high-uptake rht-type metal-organic framework decorated with acylamide groups. *J. Am. Chem. Soc.* **133**, 748–751 (2011). doi: 10.1021/ja110042b; pmid: 21174431
47. B. Li *et al.*, Enhanced binding affinity, remarkable selectivity, and high capacity of $CO_2$ by dual functionalization of a rht-type metal-organic framework. *Angew. Chem. Int. Ed.* **51**, 1412–1415 (2012). doi: 10.1002/anie.201105966
48. I. Eryazici *et al.*, Two large-pore metal-organic frameworks derived from a single polytopic strut. *Cryst. Growth Des.* **12**, 1075–1080 (2012). doi: 10.1021/cg201520z
49. J. Lu, A. Mondal, B. Moulton, M. J. Zaworotko, Polygons and faceted polyhedra and nanoporous networks. *Angew. Chem. Int. Ed.* **40**, 2113–2116 (2001). doi: 10.1002/1521-3773(20010601)40:11<2113::AID-ANIE2113>3.0.CO;2-3
50. L. Xie *et al.*, Mixed-valence iron(II, III) trimesates with open frameworks modulated by solvents. *Inorg. Chem.* **46**, 7782–7788 (2007). doi: 10.1021/ic062273m; pmid: 17696421
51. M. Kramer, U. Schwarz, S. Kaskel, Synthesis and properties of the metal-organic framework $Mo_3(BTC)_2$ (TUDMOF-1). *J. Mater. Chem.* **16**, 2245 (2006). doi: 10.1039/b601811d
52. L. J. Murray *et al.*, Highly-selective and reversible $O_2$ binding in $Cr_3(1,3,5\text{-benzenetricarboxylate})_2$. *J. Am. Chem. Soc.* **132**, 7856–7857 (2010). doi: 10.1021/ja1027925; pmid: 20481535
53. O. Kozachuk *et al.*, Solvothermal growth of a ruthenium metal-organic framework featuring HKUST-1 structure type as thin films on oxide surfaces. *Chem. Commun.* **47**, 8509–8511 (2011). doi: 10.1039/c1cc11107h; pmid: 21716991
54. N. L. Rosi *et al.*, Rod packings and metal-organic frameworks constructed from rod-shaped secondary building units. *J. Am. Chem. Soc.* **127**, 1504–1518 (2005). doi: 10.1021/ja045123o; pmid: 15686384
55. W. Zhou, H. Wu, T. Yildirim, Enhanced $H_2$ adsorption in isostructural metal-organic frameworks with open metal sites: Strong dependence of the binding strength on metal ions. *J. Am. Chem. Soc.* **130**, 15268–15269 (2008). doi: 10.1021/ja807023q; pmid: 18950163
56. K. S. Park *et al.*, Exceptional chemical and thermal stability of zeolitic imidazolate frameworks. *Proc. Natl. Acad. Sci. U.S.A.* **103**, 10186–10191 (2006). doi: 10.1073/pnas.0602439103; pmid: 16798880
57. J. H. Cavka *et al.*, A new zirconium inorganic building brick forming metal organic frameworks with exceptional stability. *J. Am. Chem. Soc.* **130**, 13850–13851 (2008). doi: 10.1021/ja8057953; pmid: 18817383
58. M. Kandiah *et al.*, Synthesis and stability of tagged UiO-66 Zr-MOFs. *Chem. Mater.* **22**, 6632–6640 (2010). doi: 10.1021/cm102601v
59. W. Morris *et al.*, Synthesis, structure, and metalation of two new highly porous zirconium metal-organic frameworks. *Inorg. Chem.* **51**, 6443–6445 (2012). doi: 10.1021/ic300825s; pmid: 22676251
60. V. Colombo *et al.*, High thermal and chemical stability in pyrazolate-bridged metal-organic frameworks with exposed metal sites. *Chem. Sci.* **2**, 1311 (2011). doi: 10.1039/c1sc00136a
61. B. Chen, N. W. Ockwig, A. R. Millward, D. S. Contreras, O. M. Yaghi, High $H_2$ adsorption in a microporous metal-organic framework with open metal sites. *Angew. Chem. Int. Ed.* **44**, 4745–4749 (2005). doi: 10.1002/anie.200462787
62. S. Horike, M. Dincă, K. Tamaki, J. R. Long, Size-selective Lewis acid catalysis in a microporous metal-organic framework with exposed $Mn^{2+}$ coordination sites. *J. Am. Chem. Soc.* **130**, 5854–5855 (2008). doi: 10.1021/ja800669j; pmid: 18399629
63. D. Britt, H. Furukawa, B. Wang, T. G. Glover, O. M. Yaghi, Highly efficient separation of carbon dioxide by a metal-organic framework replete with open metal sites. *Proc. Natl. Acad. Sci. U.S.A.* **106**, 20637–20640 (2009). doi: 10.1073/pnas.0909718106; pmid: 19948967
64. K. K. Tanabe, S. M. Cohen, Postsynthetic modification of metal-organic frameworks—A progress report. *Chem. Soc. Rev.* **40**, 498–519 (2011). doi: 10.1039/c0cs00031k; pmid: 21103601
65. S. M. Cohen, Postsynthetic methods for the functionalization of metal-organic frameworks. *Chem. Rev.* **112**, 970–1000 (2012). doi: 10.1021/cr200179u; pmid: 21916418
66. Z. Wang, K. K. Tanabe, S. M. Cohen, Tuning hydrogen sorption properties of metal-organic frameworks by postsynthetic covalent modification. *Chemistry* **16**, 212–217 (2010). doi: 10.1002/chem.200902158 pmid: 19918824
67. C.-D. Wu, A. Hu, L. Zhang, W. Lin, A homochiral porous metal-organic framework for highly enantioselective heterogeneous asymmetric catalysis. *J. Am. Chem. Soc.* **127**, 8940–8941 (2005). doi: 10.1021/ja052431t; pmid: 15969557
68. K. K. Tanabe, S. M. Cohen, Engineering a metal-organic framework catalyst by using postsynthetic modification. *Angew. Chem. Int. Ed.* **48**, 7424–7427 (2009). doi: 10.1002/anie.200903433
69. W. Morris, C. J. Doonan, H. Furukawa, R. Banerjee, O. M. Yaghi, Crystals as molecules: Postsynthesis covalent functionalization of zeolitic imidazolate frameworks. *J. Am. Chem. Soc.* **130**, 12626–12627 (2008). doi: 10.1021/ja805222x; pmid: 18754585
70. J. Lee *et al.*, Metal-organic framework materials as catalysts. *Chem. Soc. Rev.* **38**, 1450–1459 (2009). doi: 10.1039/b807080f; pmid: 19384447
71. L. Alaerts *et al.*, Probing the Lewis acidity and catalytic activity of the metal-organic framework $[Cu_3(BTC)_2]$ (BTC = benzene-1,3,5-tricarboxylate). *Chemistry* **12**, 7353–7363 (2006). doi: 10.1002/chem.200600220; pmid: 16881030
72. A. Henschel, K. Gedrich, R. Kraehnert, S. Kaskel, Catalytic properties of MIL-101. *Chem. Commun.* **2008**, 4192–4194 (2008). doi: 10.1039/b718371b; pmid: 18802526
73. A. Phan, A. U. Czaja, F. Gándara, C. B. Knobler, O. M. Yaghi, Metal-organic frameworks of vanadium as catalysts for conversion of methane to acetic acid. *Inorg. Chem.* **50**, 7388–7390 (2011). doi: 10.1021/ic201396m; pmid: 21766786
74. Y. Lu *et al.*, A cobalt(II)-containing metal-organic framework showing catalytic activity in oxidation reactions. *Z. Anorg. Allg. Chem.* **634**, 2411–2417 (2008). doi: 10.1002/zaac.200800158
75. B. Xiao, H. Hou, Y. Fan, Catalytic applications of CuII-containing MOFs based on N-heterocyclic ligand in the oxidative coupling of 2,6-dimethylphenol. *J. Organomet. Chem.* **692**, 2014–2020 (2007). doi: 10.1016/j.jorganchem.2007.01.010
76. K. S. Suslick *et al.*, Microporous porphyrin solids. *Acc. Chem. Res.* **38**, 283–291 (2005). doi: 10.1021/ar040173j; pmid: 15835875
77. B.-Q. Ma, K. L. Mulfort, J. T. Hupp, Microporous pillared paddle-wheel frameworks based on mixed-ligand coordination of zinc ions. *Inorg. Chem.* **44**, 4912–4914 (2005). doi: 10.1021/ic050452i; pmid: 15998017
78. M. H. Alkordi, Y. Liu, R. W. Larsen, J. F. Eubank, M. Eddaoudi, Zeolite-like metal-organic frameworks as platforms for applications on metalloporphyrin-based catalysts. *J. Am. Chem. Soc.* **130**, 12639–12641 (2008). doi: 10.1021/ja804703w; pmid: 18759392
79. N. V. Maksimchuk *et al.*, Heterogeneous selective oxidation catalysts based on coordination polymer MIL-101 and transition metal-substituted polyoxometalates. *J. Catal.* **257**, 315–323 (2008). doi: 10.1016/j.jcat.2008.05.014
80. C.-Y. Sun *et al.*, Highly stable crystalline catalysts based on a microporous metal-organic framework and polyoxometalates. *J. Am. Chem. Soc.* **131**, 1883–1888 (2009). doi: 10.1021/ja807357r; pmid: 19146450
81. Y. K. Hwang *et al.*, Amine grafting on coordinatively unsaturated metal centers of MOFs: Consequences for catalysis and metal encapsulation. *Angew. Chem. Int. Ed.* **47**, 4144–4148 (2008). doi: 10.1002/anie.200705998
82. B. Yuan, Y. Pan, Y. Li, B. Yin, H. Jiang, A highly active heterogeneous palladium catalyst for the Suzuki-Miyaura and Ullmann coupling reactions of aryl chlorides in aqueous media. *Angew. Chem. Int. Ed.* **49**, 4054–4058 (2010). doi: 10.1002/anie.201000576
83. C. Wang, K. E. deKrafft, W. Lin, Pt nanoparticles@ photoactive metal-organic frameworks: Efficient hydrogen evolution via synergistic photoexcitation and electron injection. *J. Am. Chem. Soc.* **134**, 7211–7214 (2012). doi: 10.1021/ja300539p; pmid: 22486151
84. N. L. Rosi *et al.*, Hydrogen storage in microporous metal-organic frameworks. *Science* **300**, 1127–1129 (2003). doi: 10.1126/science.1083440; pmid: 12750515
85. M. P. Suh, H. J. Park, T. K. Prasad, D.-W. Lim, Hydrogen storage in metal-organic frameworks. *Chem. Rev.* **112**, 782–835 (2012). doi: 10.1021/cr200274s; pmid: 22191516
86. J. L. C. Rowsell, O. M. Yaghi, Effects of functionalization, catenation, and variation of the metal oxide and organic linking units on the low-pressure hydrogen adsorption properties of metal-organic frameworks. *J. Am. Chem. Soc.* **128**, 1304–1315 (2006). doi: 10.1021/ja056639q; pmid: 16433549
87. A. G. Wong-Foy, A. J. Matzger, O. M. Yaghi, Exceptional $H_2$ saturation uptake in microporous metal-organic frameworks. *J. Am. Chem. Soc.* **128**, 3494–3495 (2006). doi: 10.1021/ja058213h; pmid: 16536503
88. B. Chen *et al.*, Surface interactions and quantum kinetic molecular sieving for $H_2$ and $D_2$ adsorption on a mixed metal-organic framework material. *J. Am. Chem. Soc.* **130**, 6411–6423 (2008). doi: 10.1021/ja710144k; pmid: 18435535
89. S. S. Han, W. A. Goddard III, Lithium-doped metal-organic frameworks for reversible $H_2$ storage at ambient temperature. *J. Am. Chem. Soc.* **129**, 8422–8423 (2007). doi: 10.1021/ja072599+; pmid: 17569539

90. K. L. Mulfort, O. K. Farha, C. L. Stern, A. A. Sarjeant, J. T. Hupp, Post-synthesis alkoxide formation within metal-organic framework materials: A strategy for incorporating highly coordinatively unsaturated metal ions. *J. Am. Chem. Soc.* **131**, 3866–3868 (2009). doi: 10.1021/ja809954r; pmid: 19292487
91. M. Dincă, J. R. Long, High-enthalpy hydrogen adsorption in cation-exchanged variants of the microporous metal-organic framework $Mn_3[(Mn_4Cl)_3(BTT)_8(CH_3OH)_{10}]_2$. *J. Am. Chem. Soc.* **129**, 11172–11176 (2007). doi: 10.1021/ja072871f; pmid: 17705485
92. Mercedes-Benz F125; www.emercedesbenz.com/autos/mercedes-benz/concept-vehicles/mercedes-benz-f125-research-vehicle-technology.
93. S. Noro, S. Kitagawa, M. Kondo, K. Seki, A new, methane adsorbent, porous coordination polymer $[CuSiF_6(4,4'\text{-bipyridine})_{2n}]$. *Angew. Chem. Int. Ed.* **39**, 2081–2084 (2000). doi: 10.1002/1521-3773(20000616)39:12<2081::AID-ANIE2081>3.0.CO;2-A
94. Green Car Congress; www.greencarcongress.com/2010/10/basf-develops-method-for-industrial-scale-mof-synthesis-trials-underway-in-natural-gas-vehicle-tanks.html.
95. A. R. Millward, O. M. Yaghi, Metal-organic frameworks with exceptionally high capacity for storage of carbon dioxide at room temperature. *J. Am. Chem. Soc.* **127**, 17998–17999 (2005). doi: 10.1021/ja0570032; pmid: 16366539
96. P. L. Llewellyn *et al.*, High uptakes of $CO_2$ and $CH_4$ in mesoporous metal-organic frameworks MIL-100 and MIL-101. *Langmuir* **24**, 7245–7250 (2008). doi: 10.1021/la800227x; pmid: 18355101
97. S. R. Caskey, A. G. Wong-Foy, A. J. Matzger, Dramatic tuning of carbon dioxide uptake via metal substitution in a coordination polymer with cylindrical pores. *J. Am. Chem. Soc.* **130**, 10870–10871 (2008). doi: 10.1021/ja8036096; pmid: 18661979
98. T. M. McDonald, D. M. D'Alessandro, R. Krishna, J. R. Long, Enhanced carbon dioxide capture upon incorporation of *N,N'*-dimethylethylenediamine in the metal-organic framework CuBTTri. *Chem. Sci.* **2**, 2022 (2011). doi: 10.1039/c1sc00354b
99. J. J. Gassensmith *et al.*, Strong and reversible binding of carbon dioxide in a green metal-organic framework. *J. Am. Chem. Soc.* **133**, 15312–15315 (2011). doi: 10.1021/ja206525x; pmid: 21877735
100. R. Matsuda *et al.*, Highly controlled acetylene accommodation in a metal-organic microporous material. *Nature* **436**, 238–241 (2005). doi: 10.1038/nature03852; pmid: 16015325
101. W. Morris, C. J. Doonan, O. M. Yaghi, Postsynthetic modification of a metal-organic framework for stabilization of a hemiaminal and ammonia uptake. *Inorg. Chem.* **50**, 6853–6855 (2011). doi: 10.1021/ic200744y; pmid: 21711030
102. B. Chen *et al.*, A microporous metal-organic framework for gas-chromatographic separation of alkanes. *Angew. Chem. Int. Ed.* **45**, 1390–1393 (2006). doi: 10.1002/anie.200502844
103. E. D. Bloch *et al.*, Hydrocarbon separations in a metal-organic framework with open iron(II) coordination sites. *Science* **335**, 1606–1610 (2012). doi: 10.1126/science.1217544; pmid: 22461607
104. M. Yoon, K. Suh, S. Natarajan, K. Kim, Proton conduction in metal-organic frameworks and related modularly built porous solids. *Angew. Chem. Int. Ed.* **52**, 2688–2700 (2013). doi: 10.1002/anie.201206410
105. Y. Nagao, R. Ikeda, S. Kanda, Y. Kubozono, H. Kitagawa, Complex-plane impedance study on a hydrogen-doped copper coordination polymer: *N,N'*-bis-(2-hydroxyethyl) dithiooxamidato-copper(II). *Mol. Cryst. Liq. Cryst.* **379**, 89–94 (2002). doi: 10.1080/713738672
106. A. Shigematsu, T. Yamada, H. Kitagawa, Wide control of proton conductivity in porous coordination polymers. *J. Am. Chem. Soc.* **133**, 2034–2036 (2011). doi: 10.1021/ja109810w; pmid: 21284399
107. J. M. Taylor, K. W. Dawson, G. K. H. Shimizu, A water-stable metal-organic framework with highly acidic pores for proton-conducting applications. *J. Am. Chem. Soc.* **135**, 1193–1196 (2013). doi: 10.1021/ja310435e; pmid: 23305324
108. T. Yamada, M. Sadakiyo, H. Kitagawa, High proton conductivity of one-dimensional ferrous oxalate dihydrate. *J. Am. Chem. Soc.* **131**, 3144–3145 (2009). doi: 10.1021/ja808681m; pmid: 19226139
109. Q. Li, R. He, J. O. Jensen, N. J. Bjerrum, Approaches and recent development of polymer electrolyte membranes for fuel cells operating above 100°C. *Chem. Mater.* **15**, 4896–4915 (2003). doi: 10.1021/cm0310519
110. J. A. Hurd *et al.*, Anhydrous proton conduction at 150°C in a crystalline metal-organic framework. *Nat. Chem.* **1**, 705–710 (2009). doi: 10.1038/nchem.402; pmid: 21124357
111. S. Bureekaew *et al.*, One-dimensional imidazole aggregate in aluminium porous coordination polymers with high proton conductivity. *Nat. Mater.* **8**, 831–836 (2009). doi: 10.1038/nmat2526; pmid: 19734885
112. D. Umeyama, S. Horike, M. Inukai, Y. Hijikata, S. Kitagawa, Confinement of mobile histamine in coordination nanochannels for fast proton transfer. *Angew. Chem. Int. Ed.* **50**, 11706–11709 (2011). doi: 10.1002/anie.201102997
113. N. Stock, S. Biswas, Synthesis of metal-organic frameworks (MOFs): Routes to various MOF topologies, morphologies, and composites. *Chem. Rev.* **112**, 933–969 (2012). doi: 10.1021/cr200304e; pmid: 22098087
114. D. Bradshaw, A. Garai, J. Huo, Metal-organic framework growth at functional interfaces: Thin films and composites for diverse applications. *Chem. Soc. Rev.* **41**, 2344–2381 (2012). doi: 10.1039/c1cs15276a pmid: 22182916
115. M. Shah, M. C. McCarthy, S. Sachdeva, A. K. Lee, H.-K. Jeong, Current status of metal-organic framework membranes for gas separations: Promises and challenges. *Ind. Eng. Chem. Res.* **51**, 2179–2199 (2012). doi: 10.1021/ie202038m
116. L. Huang *et al.*, Synthesis, morphology control, and properties of porous metal-organic coordination polymers. *Microporous Mesoporous Mater.* **58**, 105–114 (2003). doi: 10.1016/S1387-1811(02)00609-1
117. J. Cravillon *et al.*, Rapid room-temperature synthesis and characterization of nanocrystals of a prototypical zeolitic imidazolate framework. *Chem. Mater.* **21**, 1410–1412 (2009). doi: 10.1021/cm900166h
118. J. Cravillon *et al.*, Controlling zeolitic imidazolate framework nano- and microcrystal formation: Insight into crystal growth by time-resolved in situ static light scattering. *Chem. Mater.* **23**, 2130–2141 (2011). doi: 10.1021/cm103571y
119. M. Pang *et al.*, Highly monodisperse M(III)-based soc-MOFs (M = In and Ga) with cubic and truncated cubic morphologies. *J. Am. Chem. Soc.* **134**, 13176–13179 (2012). doi: 10.1021/ja3049282; pmid: 22812681
120. A. Umemura *et al.*, Morphology design of porous coordination polymer crystals by coordination modulation. *J. Am. Chem. Soc.* **133**, 15506–15513 (2011). doi: 10.1021/ja204233q; pmid: 21861521
121. M. Grzelczak, J. Vermant, E. M. Furst, L. M. Liz-Marzán, Directed self-assembly of nanoparticles. *ACS Nano* **4**, 3591–3605 (2010). doi: 10.1021/nn100869j; pmid: 20568710
122. N. Yanai, S. Granick, Directional self-assembly of a colloidal metal-organic framework. *Angew. Chem. Int. Ed.* **51**, 5638–5641 (2012). doi: 10.1002/anie.201109132
123. G. Lu, C. Cui, W. Zhang, Y. Liu, F. Huo, Synthesis and self-assembly of monodispersed metal-organic framework microcrystals. *Chem. Asian J.* **8**, 69–72 (2013). doi: 10.1002/asia.201200754; pmid: 23065843
124. N. Yanai, M. Sindoro, J. Yan, S. Granick, Electric field-induced assembly of monodisperse polyhedral metal-organic framework crystals. *J. Am. Chem. Soc.* **135**, 34–37 (2013). doi: 10.1021/ja309361d; pmid: 23240678
125. Q. Li *et al.*, Docking in metal-organic frameworks. *Science* **325**, 855–859 (2009). doi: 10.1126/science.1175441; pmid: 19679809
126. H. Deng, M. A. Olson, J. F. Stoddart, O. M. Yaghi, Robust dynamics. *Nat. Chem.* **2**, 439–443 (2010). doi: 10.1038/nchem.654; pmid: 20489710
127. P. Vairaprakash, H. Ueki, K. Tashiro, O. M. Yaghi, Synthesis of metal-organic complex arrays. *J. Am. Chem. Soc.* **133**, 759–761 (2011). doi: 10.1021/ja1097644; pmid: 21174403
128. O. Shekhah, J. Liu, R. A. Fischer, Ch. Wöll, MOF thin films: Existing and future applications. *Chem. Soc. Rev.* **40**, 1081–1106 (2011). doi: 10.1039/c0cs00147c; pmid: 21225034
129. K. M. Choi, H. J. Jeon, J. K. Kang, O. M. Yaghi, Heterogeneity within order in crystals of a porous metal-organic framework. *J. Am. Chem. Soc.* **133**, 11920–11923 (2011). doi: 10.1021/ja204818q; pmid: 21749096
130. S. Furukawa *et al.*, Heterogeneously hybridized porous coordination polymer crystals: Fabrication of heterometallic core-shell single crystals with an in-plane rotational epitaxial relationship. *Angew. Chem. Int. Ed.* **48**, 1766–1770 (2009). doi: 10.1002/anie.200804836
131. J. A. Botas, G. Calleja, M. Sánchez-Sánchez, M. G. Orcajo, Cobalt doping of the MOF-5 framework and its effect on gas-adsorption properties. *Langmuir* **26**, 5300–5303 (2010). doi: 10.1021/la100423a; pmid: 20334392
132. J. Rabone *et al.*, An adaptable peptide-based porous material. *Science* **329**, 1053–1057 (2010). doi: 10.1126/science.1190672; pmid: 20798314
133. S.-T. Zheng *et al.*, Multicomponent self-assembly of a nested $Co_{24}@Co_{48}$ metal-organic polyhedral framework. *Angew. Chem. Int. Ed.* **50**, 8034–8037 (2011). doi: 10.1002/anie.201103155
134. F. Bu *et al.*, Two zeolite-type frameworks in one metal-organic framework with $Zn_{24}@Zn_{104}$ cube-in-sodalite architecture. *Angew. Chem. Int. Ed.* **51**, 8538–8541 (2012). doi: 10.1002/anie.201203425


**Acknowledgments:** We acknowledge the original contributions made by members of the Yaghi research group as cited in the references. In particular, preliminary work on this manuscript was done by W. Morris, F. Gándara, H. Deng, and Y. Zhang. Supported by BASF SE (Ludwigshafen, Germany); U.S. Department of Energy, Office of Science, Office of Basic Energy Sciences, Energy Frontier Research Center grant DE-SC0001015; U.S. Department of Defense, Defense Threat Reduction Agency grant HDTRA 1-12-1-0053; and the Ministry of Education, Science and Technology (Korea), WCU Program grant NRF R-31-2008-000-10055-0.

## Supplementary Materials

www.sciencemag.org/cgi/content/full/341/6149/1230444/DC1
Materials and Methods
Figs. S1 to S8
Tables S1 to S5
References (*135*–*363*)
Related Web sites
CSD reference codes for MOFs

10.1126/science.1230444